

MicroRNA Mediation of Endothelial Inflammatory Response to Smooth Muscle Cells and Its Inhibition by Atheroprotective Shear Stress

Li-Jing Chen, Li Chuang, Yi-Hsuan Huang, Jing Zhou, Seh Hong Lim, Chih-I Lee, Wei-Wen Lin, Ting-Er Lin, Wei-Li Wang, Linyi Chen, Shu Chien, Jeng-Jiann Chiu

Rationale: In atherosclerotic lesions, synthetic smooth muscle cells (sSMCs) induce aberrant microRNA (miR) profiles in endothelial cells (ECs) under flow stagnation. Increase in shear stress induces favorable miR modulation to mitigate sSMC-induced inflammation.

Objective: To address the role of miRs in sSMC-induced EC inflammation and its inhibition by shear stress.

Methods and Results: Coculturing ECs with sSMCs under static condition causes initial increases of 4 anti-inflammatory miRs (146a/708/451/98) in ECs followed by decreases below basal levels at 7 days; the increases for miR-146a/708 peaked at 24 hours and those for miR-451/98 lasted for only 6 to 12 hours. Shear stress (12 dynes/cm²) to cocultured ECs for 24 hours augments these 4 miR expressions. In vivo, these 4 miRs are highly expressed in neointimal ECs in injured arteries under physiological levels of flow, but not expressed under flow stagnation. MiR-146a, miR-708, miR-451, and miR-98 target interleukin-1 receptor-associated kinase, inhibitor of nuclear factor- κ B kinase subunit- γ , interleukin-6 receptor, and conserved helix-loop-helix ubiquitous kinase, respectively, to inhibit nuclear factor- κ B signaling, which exerts negative feedback control on the biogenesis of these miRs. Nuclear factor-E2-related factor (Nrf)-2 is critical for shear-induction of miR-146a in cocultured ECs. Silencing either Nrf-2 or miR-146a led to increased neointima formation of injured rat carotid artery under physiological levels of flow. Overexpressing miR-146a inhibits neointima formation of rat or mouse carotid artery induced by injury or flow cessation.

Conclusions: Nrf-2-mediated miR-146a expression is augmented by atheroprotective shear stress in ECs adjacent to sSMCs to inhibit neointima formation of injured arteries. (*Circ Res.* 2015;116:1157-1169. DOI: 10.1161/CIRCRESAHA.116.305987.)

Key Words: atherosclerosis ■ endothelial cell ■ microRNA ■ shear stress ■ smooth muscle myocytes

Atherosclerosis and its complications constitute a major cause of mortality in the Western world. Dysfunction of vascular endothelial cells (ECs) adjacent to synthetic smooth muscle cells (sSMCs) is an initial step leading to atherosclerosis, which predominantly occurs at arterial branches and curvatures, where the local flow is disturbed with low shear stress.¹ sSMCs in the neointima of atherosclerotic lesions induce proinflammatory signaling and gene expression in ECs.¹ We recently demonstrated that sSMCs induce adhesion molecule E-selectin expression in ECs by producing proinflammatory cytokines interleukin (IL)-1 β

and IL-6, which activate IL-1 receptor-associated kinase (IRAK) and glycoprotein-130, respectively, and hence nuclear factor- κ B (NF- κ B).² Application of atheroprotective shear stress at 12 dynes/cm² to ECs cocultured with sSMCs inhibited these EC proinflammatory responses.^{2,3} Although sSMCs and shear stress have been shown to modulate cellular signals that affect EC gene expression at the transcription level, it is not known whether post-transcriptional regulators, for example, small noncoding RNAs, are involved in shear-regulation of gene expression and function of ECs in response to sSMCs.

Original received January 5, 2015; revision received January 22, 2015; accepted January 26, 2015. In December 2014, the average time from submission to first decision for all original research papers submitted to *Circulation Research* was 14.47 days.

From the Institute of Cellular and System Medicine, National Health Research Institutes, Miaoli, Taiwan (L.-J.C., Li Chuang, Y.-H.H., S.H.L., C.-I.L., T.-E.L., W.-L.W., J.-J.C.); Institute of Molecular Medicine (Linyi Chen) and Institute of Biomedical Engineering (J.-J.C.), National Tsing Hua University, Hsinchu, Taiwan; Department of Physiology and Pathophysiology, Basic Medical College, Peking University, Beijing, China (J.Z.); Department of Cardiology, Internal Medicine, Taichung Veterans General Hospital, Taichung, Taiwan (W.-W.L.); and Department of Bioengineering and Institute of Engineering in Medicine, University of California, San Diego, La Jolla (S.C.).

The online-only Data Supplement is available with this article at <http://circres.ahajournals.org/lookup/suppl/doi:10.1161/CIRCRESAHA.116.305987/-/DC1>.

Correspondence to Jeng-Jiann Chiu, PhD, Institute of Cellular and System Medicine, National Health Research Institutes, Miaoli 350, Taiwan. E-mail jjchiu@nhri.org.tw

© 2015 American Heart Association, Inc.

Circulation Research is available at <http://circres.ahajournals.org>

DOI: 10.1161/CIRCRESAHA.116.305987

Nonstandard Abbreviations and Acronyms

Anti-miR	anti-microRNA
CHUK	conserved helix-loop-helix ubiquitous kinase
EC	endothelial cell
IKK-γ	inhibitor of NF- κ B kinase subunit- γ
IL	interleukin
IL-6R	interleukin-6 receptor
IRAK	interleukin-1 receptor-associated kinase
KLF-2	Krüppel-like factor-2
miR	microRNA
NF-κB	nuclear factor- κ B
Nrf-2	NF-E2-related factor-2
Pre-miR	precursor microRNA
SMC	smooth muscle cell
Wt	wild-type

MicroRNAs (miRs) are small noncoding single-stranded RNAs that are critical for gene regulation at post-transcriptional level.⁴ MiRs bind to their target sites in 3'-untranslated regions (3'-UTRs) of mRNA to cause its degradation or translational repression.⁴ Several miRs have been identified to play important roles in modulating EC functions and atherosclerotic lesion development.^{5,6} Fang et al⁵ demonstrated in swine the anti-inflammatory role of miR-10a in ECs. MiR-92a and miR-712 were shown to be highly expressed in ECs in atheroprone areas to decrease the expressions of atheroprotective transcription factor Krüppel-like factor-2 (KLF-2) and tissue inhibitor of metalloproteinase-3, respectively, thus inducing atherogenesis.^{6,7} Shear stress has been shown to modulate miR expression in ECs and their functions.⁸⁻¹¹ Laminar shear stress at 12 dynes/cm² induces EC expressions of miR-19a and miR-23b, leading to EC cycle arrest.^{8,9} Pulsatile shear stress at 12 \pm 4 dynes/cm² decreases EC miR-92a expression and increases KLF-2 expression to maintain EC homeostasis.¹⁰ KLF-2 modulates shear-induction of EC miR-143/145, which can modulate SMC phenotype from synthetic toward contractile.¹¹ We recently found that shear stress applied to ECs inhibits the transmission of miR-126 from ECs to cocultured sSMCs to suppress sSMC proliferation.¹² However, it is not known whether miRs are involved in sSMC modulation of EC gene expression and function and what are the effects of shear stress on this modulation.

In this study, we found that atheroprotective shear stress augments miR-146a, miR-708, miR-451, and miR-98 expressions in ECs cocultured with sSMCs. These 4 miRs have anti-inflammatory actions by directly targeting IRAK, inhibitor of NF- κ B kinase subunit- γ (IKK- γ), IL-6 receptor (IL-6R), and conserved helix-loop-helix ubiquitous kinase (CHUK) genes, respectively, to inhibit NF- κ B signaling, which exerts negative feedback control on the biogenesis of these miRs. In vivo, these 4 miRs are highly expressed in ECs of neointimal lesions in injured rat carotid arteries under physiological levels of flow, but not expressed under flow stagnation. We also found that NF-E2-related factor (Nrf)-2 is a critical transcription factor for shear-induced miR-146a transcription in cocultured ECs. Administration of lentivirus carrying mature miR-146a (Lenti-miR-146a) inhibits neointima formation induced by

injury or flow cessation in rats or mice. Our findings suggest that miR-146a, miR-708, miR-451, and miR-98 may serve as valuable molecular targets for intervention against vascular disorders resulting from atherosclerosis and restenosis.

Methods**Cell Culture and Coculture Flow System**

Human aortic ECs and SMCs were obtained commercially (Clonetics, Palo Alto, CA). Details of cell culture procedures and EC/SMC coculture flow system are provided in Online Data Supplement.

Argonaunts 2 Complex Immunoprecipitation

ECs were collected by scraping and lysed. An anti-argonaunts 2 antibody (1 μ g/100 μ L; Cell Signaling) was added and the immune complexes were isolated with protein A/G Sepharose beads.

Chromatin Immunoprecipitation Assay

ChIP assay was performed according to the manufacturer's protocol (EZ-ChIP; Merck Millipore). All primers are listed in Online Tables I and II.

Animals

Carotid artery balloon injury was performed in male Sprague-Dawley rats (350–500 g), and carotid artery ligation was performed in female FVB/NJ mice (12 weeks of age). Animals were euthanized with 100% carbon dioxide. All animals and experiments were maintained and performed according to the guidelines of the Animal Research Committee of National Health Research Institutes.

An expanded Methods section is provided in Online Data Supplement.

Results**Atheroprotective Shear Stress Augments miR-146a, miR-708, miR-451, and miR-98 Expressions in Cocultured ECs**

Three independent groups of experiments were performed with miR arrays, that is, monocultured ECs (EC/NC), ECs cocultured with sSMCs under static condition for 24 hours (EC/SMC), and EC/SMC coculture with the subsequent exposure of ECs to shear stress at 12 dynes/cm² for 6 hours (SS EC/SMC). MiR expressions with a mean coculture/monoculture ratio \geq 2.0 (and $P \leq 0.05$) were considered positively regulated by the coculture, whereas those with a mean ratio ≤ 0.5 (and $P \leq 0.05$) were considered negatively regulated. Of the 380 miRs on the array, the expressions of miR-146a and miR-708 in ECs were significantly induced by static 24-hour coculture with sSMCs, whereas those of miR-98, miR-30b, miR-30c, miR-885, miR-149, miR-654-3p, and miR-451 were significantly decreased (Online Table III). Analysis of the time course of these 9 miR expressions by quantitative polymerase chain reaction showed that static coculture with sSMCs causes initial increases of miR-146a, miR-708, miR-451, and miR-98 expressions in ECs followed by later declines to below basal levels (Figure 1A). MiR-146a and miR-708 peaked at 24 hours, and then declined to below basal levels at 7 days; miR-451 and miR-98 declined to below basal levels at 24 hours. MiR-30b, miR-30c, miR-885, miR-149, and miR-654-3p of static cocultured ECs did not show an initial increase at 1 hour and all decreased to below basal level at 24 hours (Figure 1B).

Application of shear stress to cocultured ECs for 6 or 24 hours induced miR-146a, miR-708, miR-451, and miR-98

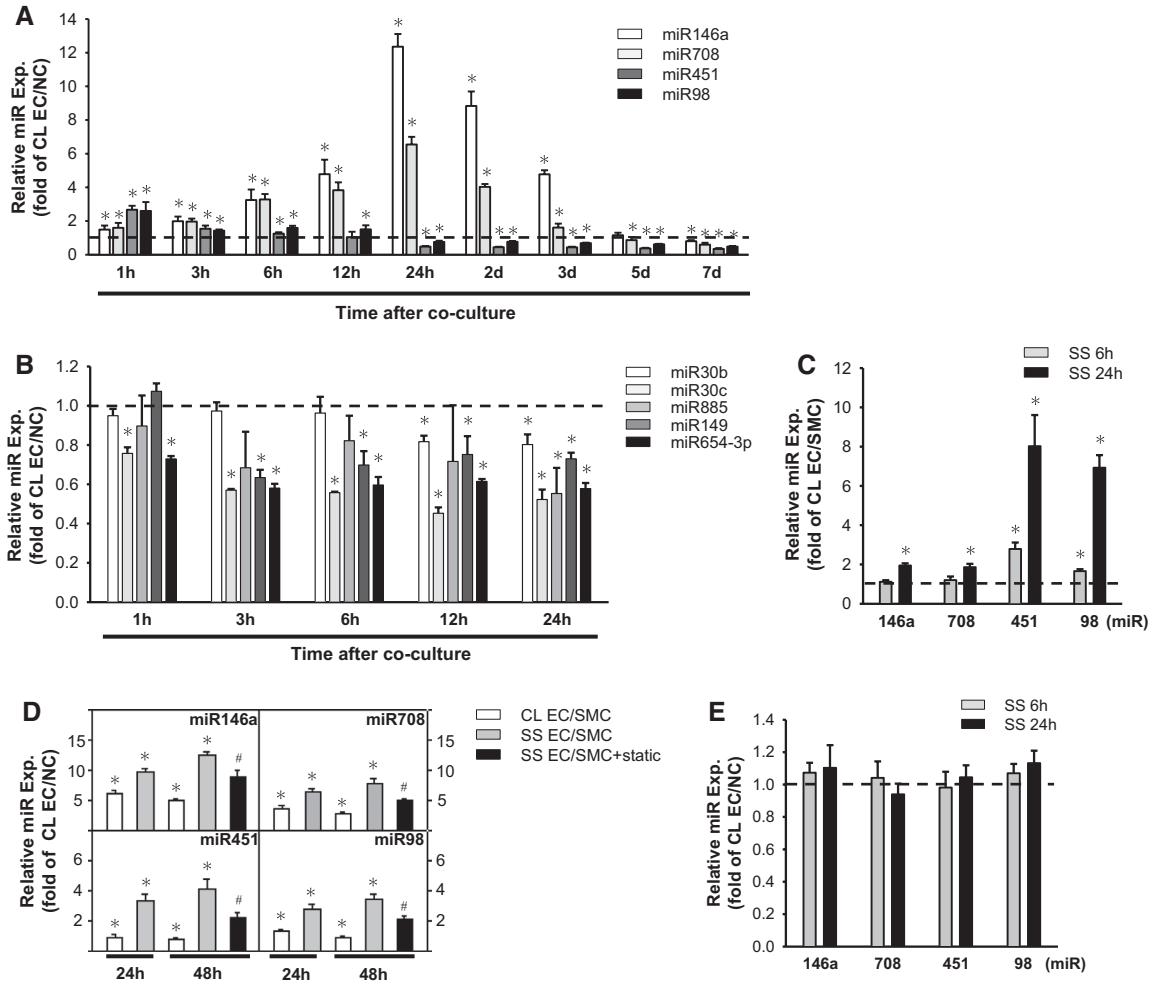


Figure 1. MiR expression profiles in cocultured endothelial cells (ECs) under static condition and in response to shear stress. **A** and **B**, ECs were cultured alone (EC/NC) or cocultured with sSMCs (EC/SMC) under static conditions (CL). The EC miR expression was examined by quantitative polymerase chain reaction. **C** and **D**, Cocultured ECs were kept under static condition or exposed to shear stress at 12 dynes/cm² (SS) for 6 hours (**C**), 24 hours (**C** and **D**), or 48 hours (**D**). Cocultured ECs were subjected to shear stress for 24 hours, followed by the flow cessation for additional 24 hours (**D**). **E**, Monocultured ECs were kept under static condition or exposed to flow for 6 or 24 hours. Data are mean±SEM from 3 independent experiments. **P*<0.05 vs CL EC/NC. #*P*<0.05 vs SS EC/SMC 48 hours. sSMC indicates synthetic smooth muscle cells.

expressions in these ECs (Online Table III; Figure 1C). These shear-inductions of EC miRs were declined by 24 hours of flow cessation, as compared with the cells exposed to continuous flow (Figure 1D). Shear stress had no effects on these 4 miR expressions in monocultured ECs (Figure 1E).

MiR-146a, miR-708, miR-451, and miR-98 Directly Target IRAK, IKK-γ, IL-6R, and CHUK Genes, Respectively

Our previous study showed that sSMCs release IL-1β and IL-6 to activate IRAK and IL-6R and hence NF-κB in adjacent ECs.² We investigated whether miR-146a, miR-708, miR-451, and miR-98 can target IRAK, IL-6R, and NF-κB relevant genes. Analysis with bioinformatics algorithms PicTar, microRNA.org, and TargetScan 4.2 identified that the 3'-UTRs of IRAK, IKK-γ, IL-6R, and CHUK genes contain the putative-binding sites (seed sequences) of miR-146a, miR-708, miR-451, and miR-98, respectively. We generated reporter constructs containing the firefly luciferase gene fused

to wild-type and mutant of putative target sites of these genes (Online Figure I). Cotransfection with wild-type constructs and precursors of respective miRs (pre-miRs) into HEK293 cells reduced luciferase activities in these cells (Figure 2A); such reductions of luciferase activities were not observed by cotransfection with the mutant constructs. Transfecting ECs with pre-miR-146a, miR-708, miR-451, and miR-98 reduced protein (Figure 2B) and mRNA (Figure 2C) levels of IRAK, IKK-γ, IL-6R, and CHUK, respectively, in comparison with control groups. Analysis of miR-induced silencing complexes immunoprecipitated with anti-argonats 2 antibody showed increased mRNA levels of these genes in pre-miR-transfected ECs (Figure 2C), indicating that these EC genes are regulated by their respective miRs at the post-transcriptional level through binding to argonats 2 in miR-induced silencing complexes. Coculturing ECs with sSMCs induced EC expressions of IRAK, IKK-γ, IL-6R, and CHUK mRNAs in miR-induced silencing complexes (Figure 2D). Such sSMC-inductions of EC genes in miR-induced silencing complexes

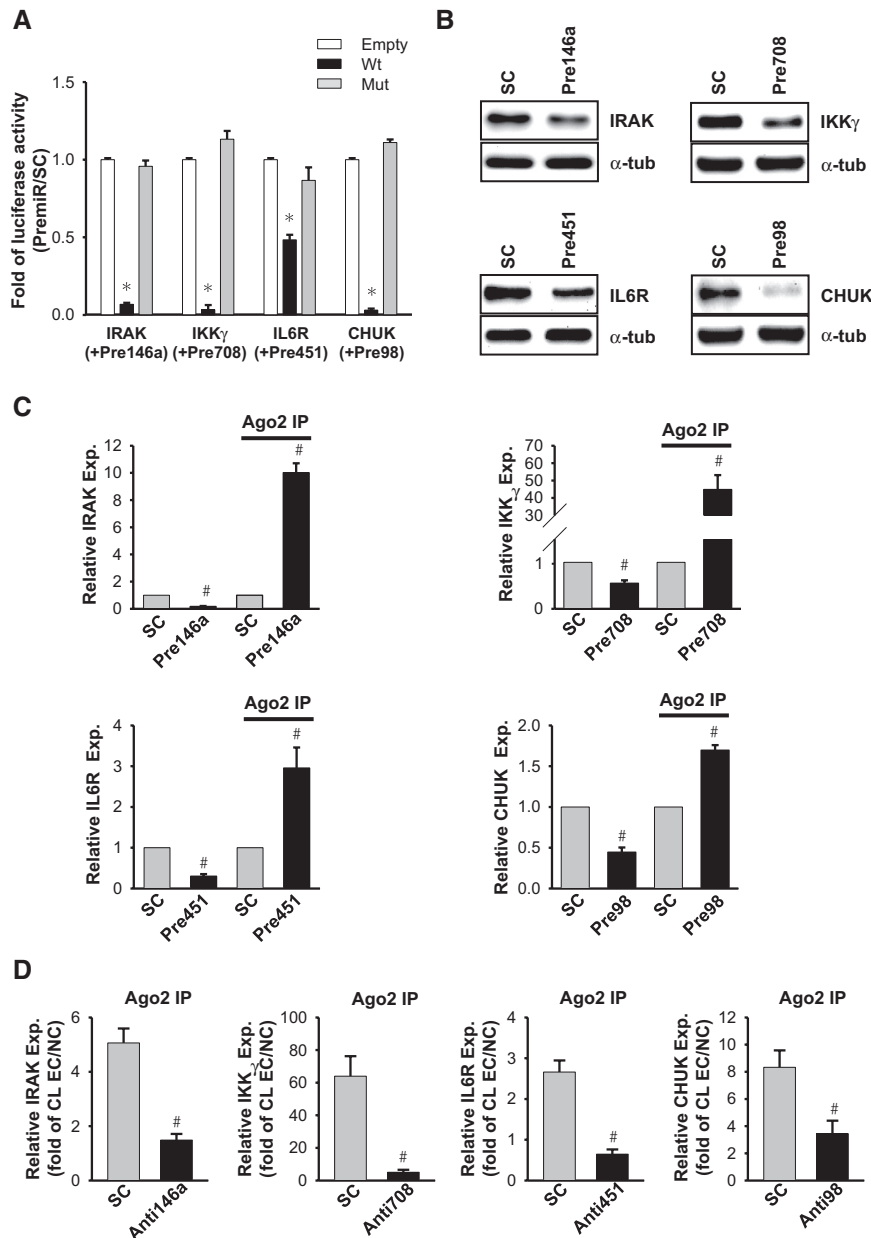


Figure 2. Direct target genes of miR-146a, miR-708, miR-451, and miR-98. **A**, Reporter constructs containing wild-type (Wt) and mutant (Mut) of putative miR target sites of indicated genes were cotransfected with the respective pre-miRs (PremiR) or a scramble control (SC) into HEK293 cells for 24 hours. **B**, Endothelial cells (ECs) were transfected with pre-miR-146a, miR-451, miR-98 (20 nmol/L each), and pre-miR-708 (0.1 nmol/L) or a SC for 24 hours. **C**, ECs were transfected with the indicated pre-miRs or a SC for 24 hours, and performed with the argonautes 2 immunoprecipitation assay. **D** ECs were transfected with anti-miR-146a, miR-708, miR-451, and miR-98 (AntimiR; 5 nmol/L each) or a SC for 24 hours, and then were cultured alone (CL EC/NC) or cocultured with synthetic smooth muscle cells for 12 hours. * $P < 0.05$ vs empty vector. # $P < 0.05$ vs SC. **A**, **C**, and **D**, Data are mean \pm SEM from 3 independent experiments. **B**, Results are representative of triplicate experiments with similar results. Ago2 indicates argonautes 2; CHUK, conserved helix-loop-helix ubiquitous kinase; IKK- γ , inhibitor of NF- κ B kinase subunit- γ ; IL6R, interleukin-6 receptor; and IRAK, interleukin-1 receptor-associated kinase.

were inhibited by transfecting ECs with the respective antagonists (anti-miRs).

MiR-146a, miR-708, miR-451, and miR-98 Modulate NF- κ B Signaling, Which Exerts Negative Feedback Control on the Biogenesis of These miRs in Cocultured ECs

Static coculturing ECs with sSMCs induced p65 and I κ B α phosphorylations in ECs during the 24-hour period test (Figure 3A). Such sSMC-activations of EC p65 and I κ B α

were reduced after 1 hour of flow exposure. Overexpressing optimal concentrations of pre-miR-146a, miR-451, miR-98 (20 nmol/L each), and miR-708 (1 nmol/L) in ECs also reduced sSMC-activations of EC I κ B α (Figure 3B) and p65 (Figure 3C). These effects of EC pre-miR overexpression were negated by the respective anti-miRs (Figure 3C; Online Figure II). Coculturing ECs with sSMCs induced EC E-selectin expression (Figure 3D) and monocyte adhesion (Figure 3E). These sSMC-induced responses were inhibited by overexpressing ECs with the 4 pre-miRs, but anti-miRs had no effect.

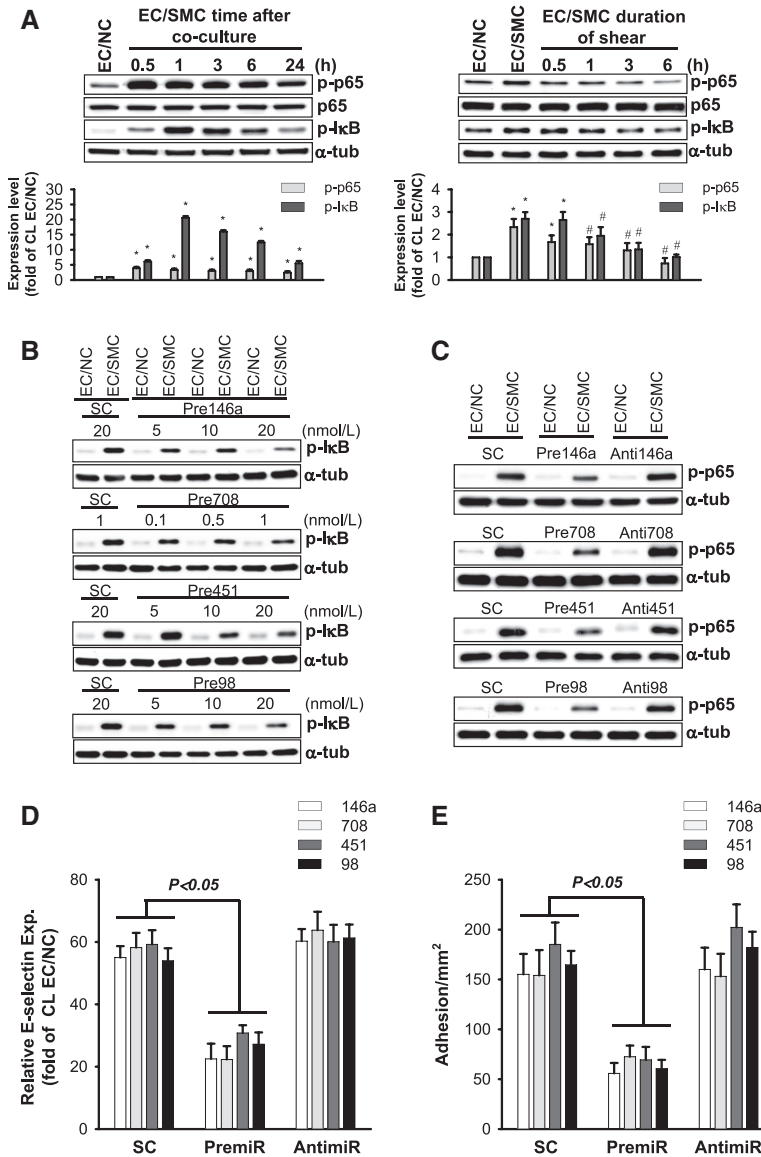


Figure 3. MiR inhibition in synthetic smooth muscle cells (sSMC)-induced proinflammatory responses in cocultured endothelial cells (ECs). **A**, ECs were cultured alone (EC/NC) or cocultured with sSMCs (EC/SMC) under static condition (CL). In parallel experiments, ECs cocultured with SMCs for 24 hours were subjected to shear stress. The p65 and IκBα phosphorylation levels were determined by Western blot. **P*<0.05 vs CL EC/NC. #*P*<0.05 vs CL EC/SMC. **B** and **C**, ECs were transfected with the designated pre- or anti-miRs or a scramble control at the indicated concentrations (**B**) or the optimal concentrations (**C**) for 24 hours. **D**, The E-selectin mRNA expression in cocultured ECs was quantified by quantitative polymerase chain reaction. **E**, The monocyte adhesion assay was performed. **A**, **D**, and **E**, Data are mean±SEM from 3 independent experiments. **B** and **C**, Results are representative of triplicate experiments with similar results.

sSMC-inductions of EC miR-146a, miR-708, miR-451, and miR-98 were inhibited by transfecting ECs with p65-specific siRNA (Figure 4A) and by pretreatment with the specific phospho-IκB inhibitor BAY117082 (Figure 4B). Coculturing ECs with sSMCs induced time-dependent induction of EC primary miR-146a (Figure 4C), whose promoter region contains 3 NF-κB-binding sites.¹³ Coculture of sSMCs with ECs transfected with the constructs containing promoter region of miR-146a (547 bp) and reporter gene luciferase induced luciferase activities (Figure 4D). These responses were not seen when ECs were transfected with the constructs containing mutated NF-κB-binding sites (Figure 4D). Chromatin immunoprecipitation assays using anti-p65 antibody and NF-κB-specific primers for miR-146a promoter showed that sSMC-coculture induced NF-κB binding to miR-146a promoter region (Figure 4E). Taken together, our results indicate that increased activation of NF-κB in ECs cocultured with sSMCs induces EC biogenesis of miR-146a, miR-708, miR-451, and miR-98, which in turn target NF-κB signaling to cause declined expression of these miRs in cocultured ECs.

Nrf-2 is Critical for Shear-Induction of miR-146a in Cocultured ECs

The promoter region of miR-146a contains 4 putative-binding sites for Nrf-2 (sequence: TGActcAGCa; Online Figure III), which was shown to be activated by shear stress.¹⁴ We investigated whether Nrf-2 is involved in shear-induction of miR-146a in cocultured ECs. Nuclear fractionation assay showed that shear stress applied to cocultured ECs induces Nrf-2 translocation into EC nuclei (Figure 5A). Electrophoretic mobility shift assay (Figure 5B) and chromatin immunoprecipitation assay (Figure 5C) demonstrated that shear stress increases Nrf-2-binding activity in cell-free system and Nrf-2 binding to miR-146a promoter region in EC nuclei. As controls, coculturing ECs with sSMCs under static condition did not induce these responses. We further generated a mutant construct containing the promoter region of miR-146a, with a mutation in Nrf-2-binding site (at -193 bp). Application of shear stress to cocultured ECs transfected with a wild-type construct induced a 2.2-fold

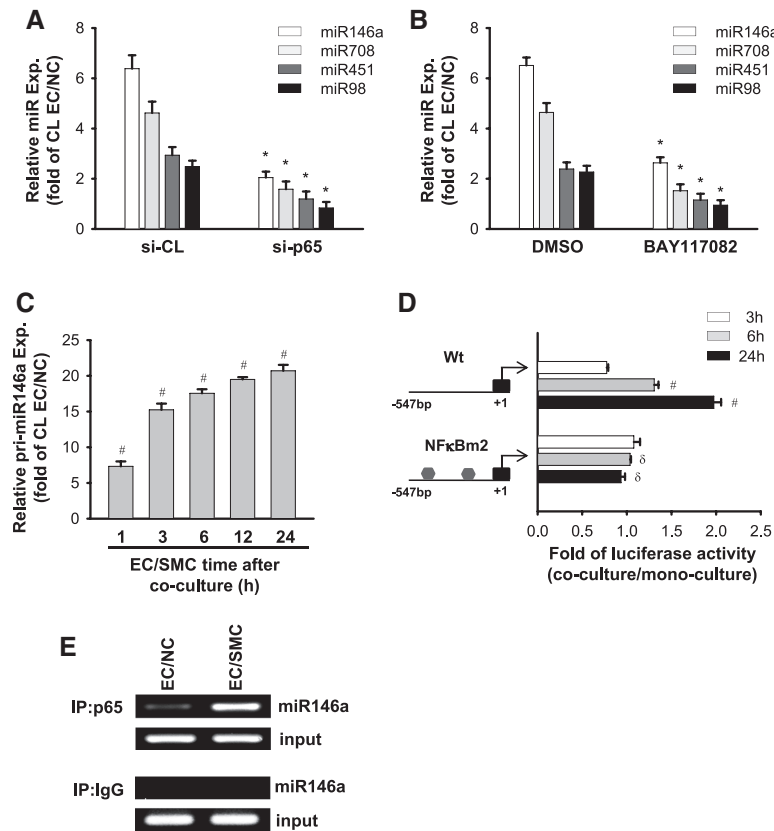


Figure 4. Nuclear factor (NF)-κB is critical for synthetic smooth muscle cells (sSMC)-induction of miRs in endothelial cells (ECs). **A**, ECs were transfected with control (siCL) or p65-specific siRNA (sip65; 20 nmol/L). **B**, Cells were pretreated with dimethyl sulfoxide (DMSO) or BAY117082 for 1 hour. These ECs were kept under static condition or cocultured with sSMCs for 6 hours (for miR-451/98) or 12 hours (for miR-146a/708). **C**, The expression of pri-miR-146a in cocultured ECs was determined by quantitative polymerase chain reaction. **D**, Wild-type (Wt) promoter construct (–547 bp) of miR-146a and its mutant at 2 putative NF-κB-binding sites (NFκBm2) were transfected into ECs. **E**, ECs were cultured alone or cocultured with sSMCs under static conditions for 12 hours, and chromatin immunoprecipitation assay was performed. **P*<0.05 vs siCL or DMSO. #*P*<0.05 vs CL EC/NC. δ*P*<0.05 vs Wt. **A** to **D**, Data are mean±SEM from 3 independent experiments. **E**, Results are representative of triplicate experiments with similar results.

increase in luciferase activity in comparison with static control cells (Figure 5D). This shear-induced response was absent in ECs transfected with mutant constructs. Transfecting cocultured ECs with Nrf-2-specific siRNA (compared with control siRNA, 20 nmol/L each) inhibited shear-inductions of miR-146a and miR-708, but not miR-451 and miR-98 (Figure 5E) in these ECs. Treatment of cocultured ECs with a specific Nrf-2 activator sulforaphane (10 μmol/L) under static condition for 24 hours can mimic shear stress effects to induce Nrf-2 binding to the promoter region of miR-146a (Figure 5F) and its promoter activity (Figure 5G) and hence expression (Figure 5H) in these ECs. However, sulforaphane had no effect on EC miR-451, miR-98, and miR-708 expressions (Figure 5H). These results indicate that Nrf-2 is involved in shear-induction of miR-146a, but not miR-451, miR-98, and miR-708, in cocultured ECs.

Integrins Regulate Shear-Inductions of miR-146a, miR-708, miR-451, and miR-98 in Cocultured ECs

ECs were pretreated with poly-L-lysine (100 μg/mL) and RGDS (Arg-Gly-Asp-Ser; 500 μg/mL) for 2 hours to block the integrin-extracellular matrix interactions, and then cocultured with sSMCs under static conditions or in response to flow for 24 hours. In addition, ECs were transfected with β₁- and β₃-integrin-specific siRNAs (20 nmol/L each), which reduced the expression of the respective integrins by ≈70% (compared with control siRNA). The results showed that β₁ and β₃ integrins are involved in shear-inductions of these 4 miRs in cocultured ECs. Detailed results are provided in Online Data Supplement and Online Figure IV.

MiR-146a, miR-708, miR-451, and miR-98 are Highly Expressed in Neointimal ECs in Injured Arteries Under Physiological Levels of Flow, But Not Expressed Under Flow Stagnation

To investigate whether the SMC- and shear-modulations of miR-146a, miR-708, miR-451, and miR-98 expressions found in cultured ECs in vitro also occur in vivo, we used a rat carotid artery balloon injury model to create close interactions between ECs and sSMCs. In addition to studies under physiological levels of flow, in some experiments the affected arteries were subjected to a partial ligation (≈60% constriction of the artery diameter) at the proximal edge (Figure 6A). Ultrasonography demonstrated that this injured carotid artery model resulted in flow stagnation, with virtually no detectable level of flow velocity (Figure 6B). Hematoxylin and eosin staining showed that the intima-to-media thickness ratio of the constricted injured arteries is higher than that of unconstricted injured arteries (Figure 6C). In situ hybridization of the 4 miRs and immunohistochemical staining on Nrf-2 in serial sections of affected arteries (Figures 6D and 6E; Online Figure V) showed that these 4 miRs and Nrf-2 are not expressed in neointimal ECs in constricted injured arteries under flow stagnation. However, they are highly expressed in ECs in unconstricted injured arteries under physiological levels of flow. There was no detectable level of these 4 miRs in control vessels. These results indicate that miR-146a, miR-708, miR-451, and miR-98 are highly expressed in ECs of neointimal lesions with sSMCs in the presence of physiological levels of flow in vivo, which may play inhibitory roles in preventing neointima formation in injured arteries. These findings

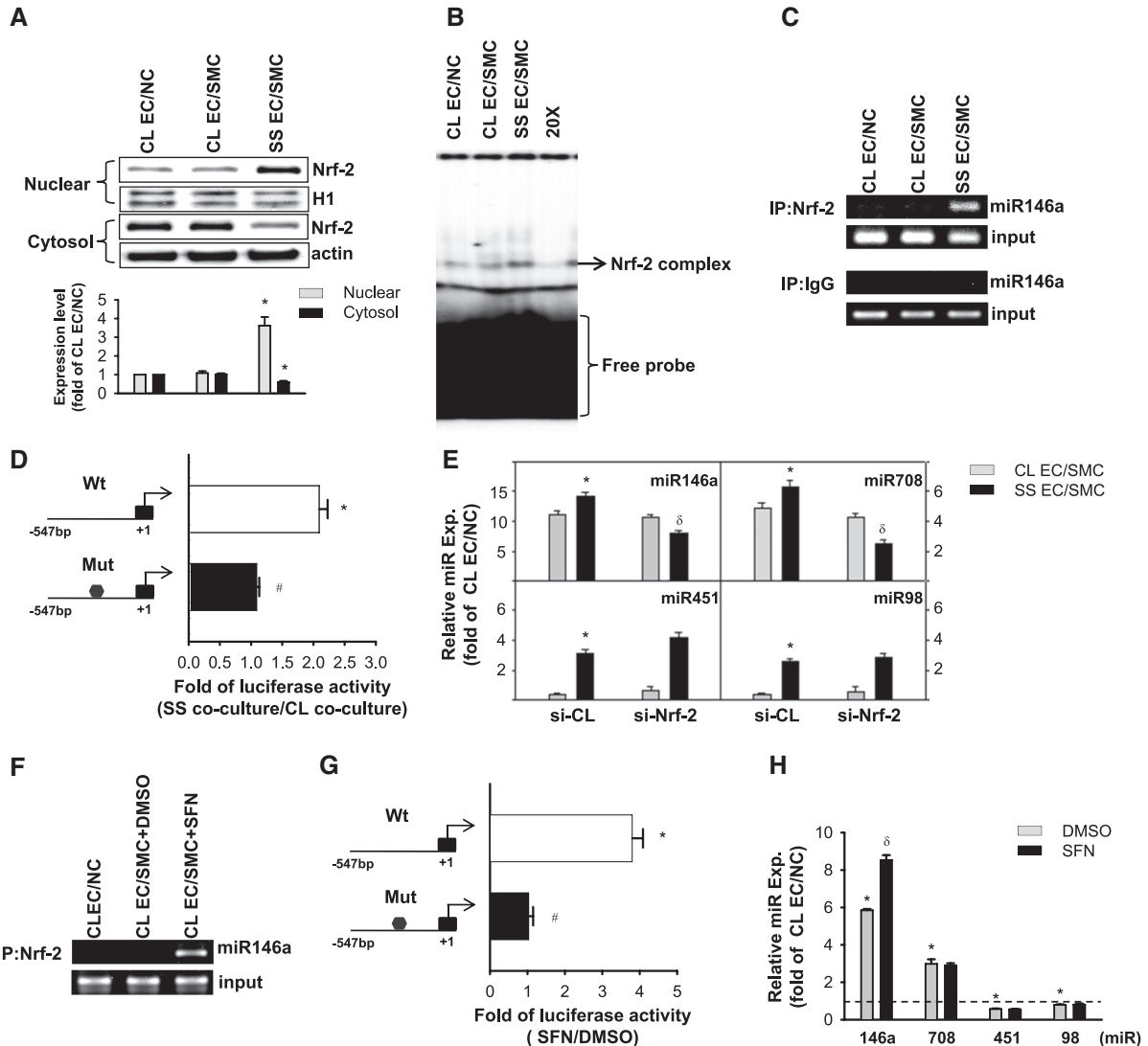


Figure 5. Nrf-2 is critical for shear-induction of miR-146a in cocultured endothelial cells (ECs). **A**, ECs were cultured alone or cocultured with synthetic smooth muscle cells (sSMCs) under static condition for 24 hours. Cocultured ECs were subjected to shear stress for 24 hours. Nrf-2 expression in the EC nuclei and cytosol was determined by Western blot. **B**, Electrophoretic mobility shift assay analysis of nuclear protein extracts from these ECs. The nuclear extracts were preincubated with excess unlabeled oligonucleotides containing Nrf-2-binding sequences (x20). **C**, Chromatin immunoprecipitation assay was performed. Input DNA was analyzed by polymerase chain reaction to normalize the extracts used for immunoprecipitation. **D**, Wild-type (Wt) promoter construct (–547 bp) of miR-146a and its mutant at the Nrf-2-binding site (Mut) were transfected into ECs. **E**, ECs were transfected with Nrf-2-specific siRNA (siNrf-2) or control siRNA (siCL), and then cultured alone or cocultured with sSMCs under static condition. The cocultured ECs were subjected to shear stress for 24 hours. **F** to **H**, Cocultured ECs were treated with dimethyl sulfoxide (DMSO) or sulforaphane (SFN; 10 μmol/L) for 24 hours. The binding of Nrf-2 to the promoter region of miR-146a (**F**) and its promoter activity (**G**) and different miR expressions (**H**) were examined. **P*<0.05 vs CL EC/SMC. #*P*<0.05 vs Wt. δ*P*<0.05 vs siCL or DMSO. **A**, **D**, **E**, **G**, and **H**, Data are mean±SEM from 3 independent experiments. **B**, **C**, and **F**, Results are representative of triplicate experiments with similar results. SS indicates shear stress.

validated our in vitro findings that increases in shear stress induce these 4 miR expressions in ECs cocultured with sSMCs.

Nrf-2 is Involved in Shear-Induction of EC miR-146a In Vivo

To investigate whether Nrf-2 is involved in shear-induction of EC miR-146a in vivo, lentiviral-mediated RNA interference was performed 2 weeks after balloon injury on carotid arteries in rats (n=5), where the denuded EC layer had recovered from injury, and the animals were euthanized after additional 2 weeks. The lentiviral-mediated Nrf-2 silencing abolishes miR-146a expression in ECs of unconstricted injured arteries

under physiological levels of flow (Figure 7A), and this is accompanied by a concomitant increase in neointima formation, in comparison with control shRNA-infected animals (n=5; Figures 7A and 7B). Administration of anti-miR-146a in unconstricted injured arteries to knockdown EC miR-146a expression (Figure 7C) also increased neointima formation (Figures 7C and 7D). In contrast, overexpressing miR-146a by using the shMIMIC strategy (see details in the next section) resulted in increased expression of miR-146a in ECs (Figure 7E) and decreased formation of neointimal lesions in constricted injured arteries under flow stagnation (Figures 7E

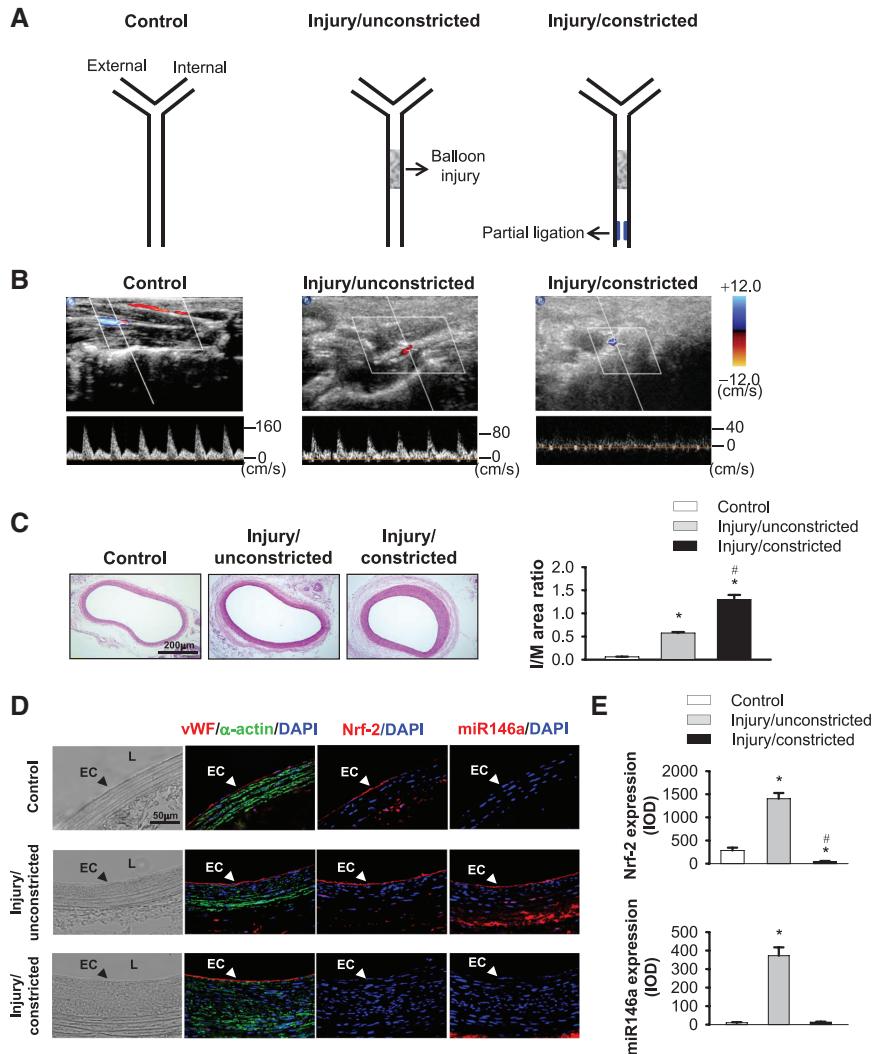


Figure 6. MiR-146a is highly expressed in the endothelial cell (EC) layer of neointimal lesions in injured arteries under flow. **A**, Schematic diagrams of rat experimental models. **B**, Ultrasound measurements on the affected carotid arteries. **Top**, Vessels with the two-dimensional and color Doppler modes. **Bottom**, Doppler spectral display of velocity profiles with a plus wave Doppler mode. **C**, Hematoxylin and eosin staining of the cross-sections of affected carotid arteries 4 weeks after surgery. I/M: intima/media ratio (n=5 each). **D**, Serial cross-sections of the affected carotid arteries (n=5 each) were stained for Nrf-2 and miR-146a expressions. L indicates lumen. **E**, Quantitative analysis of the results in **D**. * $P < 0.05$ vs control vessels. # $P < 0.05$ vs injury/unconstricted model. Images shown in each examination are representative of 5 rats with similar results. DAPI indicates 4',6-diamidino-2-phenylindole; IOD, integrated optical density; and vWF, von Willebrand factor.

and 7F). These results indicate that Nrf-2–induction of EC miR-146a under physiological levels of flow plays inhibitory roles in neointima formation in injured arteries.

Administration of Lenti-miR-146a Reduced Neointima Formation in a Mouse Carotid Artery Ligation Model

To confirm the therapeutic effect of miR-146a on neointima formation in vivo, we performed the shMIMIC lentivirus-mediated miR overexpression strategy by using a mouse carotid artery ligation model, in which neointimal lesions were created with the maintenance of endothelial integrity. Lenti-miR-146a containing mature miR-146a sequences and cDNA encoding green fluorescence protein was constructed and infected into ECs under static conditions for 24 and 48 hours (5×10^6 TU/mL each). ECs showed $\approx 70\%$ infection efficiency, as determined from the percentage of green fluorescence

protein–positive cells relative to total cells (Figure 8A). MiR-146a expression in Lenti-miR-146a–infected cells was increased by 60- to 80-folds in comparison with Lenti-null–infected cells (Figure 8B). This miR-146a overexpression resulted in $\approx 60\%$ reductions in endogenous IRAK mRNA (Figure 8C) and protein (Figure 8D) levels.

To test in vivo overexpression efficiency of Lenti-miR-146a, the Lenti-miR-146a construct (5×10^7 TU/mL in 100 μ L) was administered through the tail vein of mice (n=5) weekly after carotid artery ligation. Control animals received Lenti-null or saline injection (n=5 each). En face staining of luminal surface of the carotid arteries with an anti–green fluorescence protein antibody 2 weeks after lentivirus injection showed high levels of in vivo infection efficiency of Lenti-miR-146a and Lenti-null in intact EC layers (Online Figure VIA). In situ hybridization of arterial cross-sections (Figure 8E) and

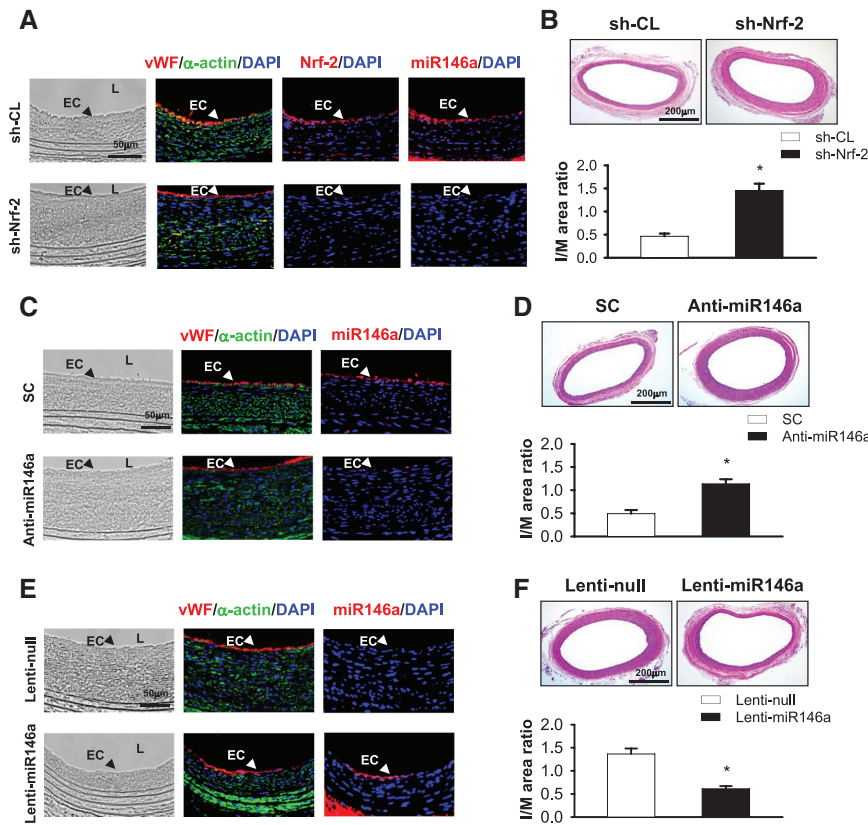


Figure 7. Nrf-2 and miR-146a play crucial roles in modulating neointimal lesion formation in vivo. Two weeks after balloon injury in unconstricted carotid arteries in rats (n=5), 50 μ L of lentiviral control (shCL) or Nrf-2-specific shRNA (shNrf-2; 1×10^6 TU/mL each; **A** and **B**), 10 μ g of chemically modified anti-miR-146a or scramble controls (SCs; **C** and **D**), or in constricted carotid arteries in rat (n=5), Lenti-null or Lenti-miR-146a (5×10^6 TU/mL each; **E** and **F**) was respectively infused into the local injured sites. The rats were euthanized 2 weeks after local injections of agents. **A**, **C**, and **E**, Serial cross-sections of the affected carotid arteries were stained for Nrf-2 and miR-146a. L indicates lumen. **B**, **D**, and **F**, Hematoxylin and eosin staining of the cross-sections of affected carotid arteries. I/M: intima/media ratio (n=5). * $P < 0.05$ vs control group. Images shown in each examination are representative of 5 rats with similar results. DAPI indicates 4',6'-diamidino-2-phenylindole; and vWF, von Willebrand factor.

en face staining (Online Figures VIB and VIC) demonstrated that miR-146a expression in intact EC layer was increased by Lenti-miR-146a injection, with concomitant decreases in IRAK expression, as compared with Lenti-null and saline groups. Ligation of left common carotid arteries in Lenti-null-infected mice (n=5) for 4 weeks increased neointimal lesion formation of the arteries (Figures 8F and 8G). This increased neointima formation in ligated arteries was inhibited by lentivirus-mediated miR-146a overexpression, confirming the inhibitory role of miR-146a in arterial neointima formation in vivo.

Discussion

This study has identified miR-146a, miR-708, miR-451, and miR-98 as novel anti-inflammatory miRs in ECs cocultured with sSMCs; the expression of these miRs is sustainably induced by atheroprotective shear stress. MiR-146a, miR-708, miR-451, and miR-98 directly target IRAK, IKK- γ , IL-6R, and CHUK genes, respectively, to inhibit NF- κ B signaling, which exerts negative feedback control on the biogenesis of these 4 miRs (summarized in Figure 8H). Shear-induction of these miRs in cocultured ECs is mediated by β_1 and β_3 integrins. In addition, miR-146a is regulated by Nrf-2 at the transcriptional level in response to flow. Previous studies using

EC monocultures have identified EC miR-712,⁷ miR-19a,⁸ miR-23b,⁹ miR-92a,¹⁰ miR-143/145¹¹, and miR-21¹⁵ as shear-responsive miRs that play functional roles. Our study using EC/SMC coculture system has shown the novel results that EC miR-146a, miR-708, miR-451, and miR-98 can be augmented by atheroprotective shear stress in close adjacency to sSMCs to serve as negative regulators for sSMC-induced EC inflammation. These miRs may serve as therapeutic molecules against vascular disorders resulting from atherosclerosis and restenosis.

The induction of anti-inflammatory miR-146a, miR-708, miR-451, and miR-98 in ECs by static coculture with sSMCs may be considered as a compensatory response for ECs against sSMC-induced inflammation. However, this sSMC-induction of these 4 miRs is declined when the duration of coculture is lengthened, suggesting a limitation of the compensatory response of static ECs in the face of sustained action from sSMCs. Application of shear stress to cocultured ECs for 24 hours induces these 4 miR expressions in comparison with static cocultured ECs. This shear-induction of these 4 miRs was declined by flow cessation in comparison with continuous flow. In vivo, these 4 miRs are not expressed in ECs of neointimal lesions in injured arteries under flow stagnation, but become highly expressed under physiological levels of

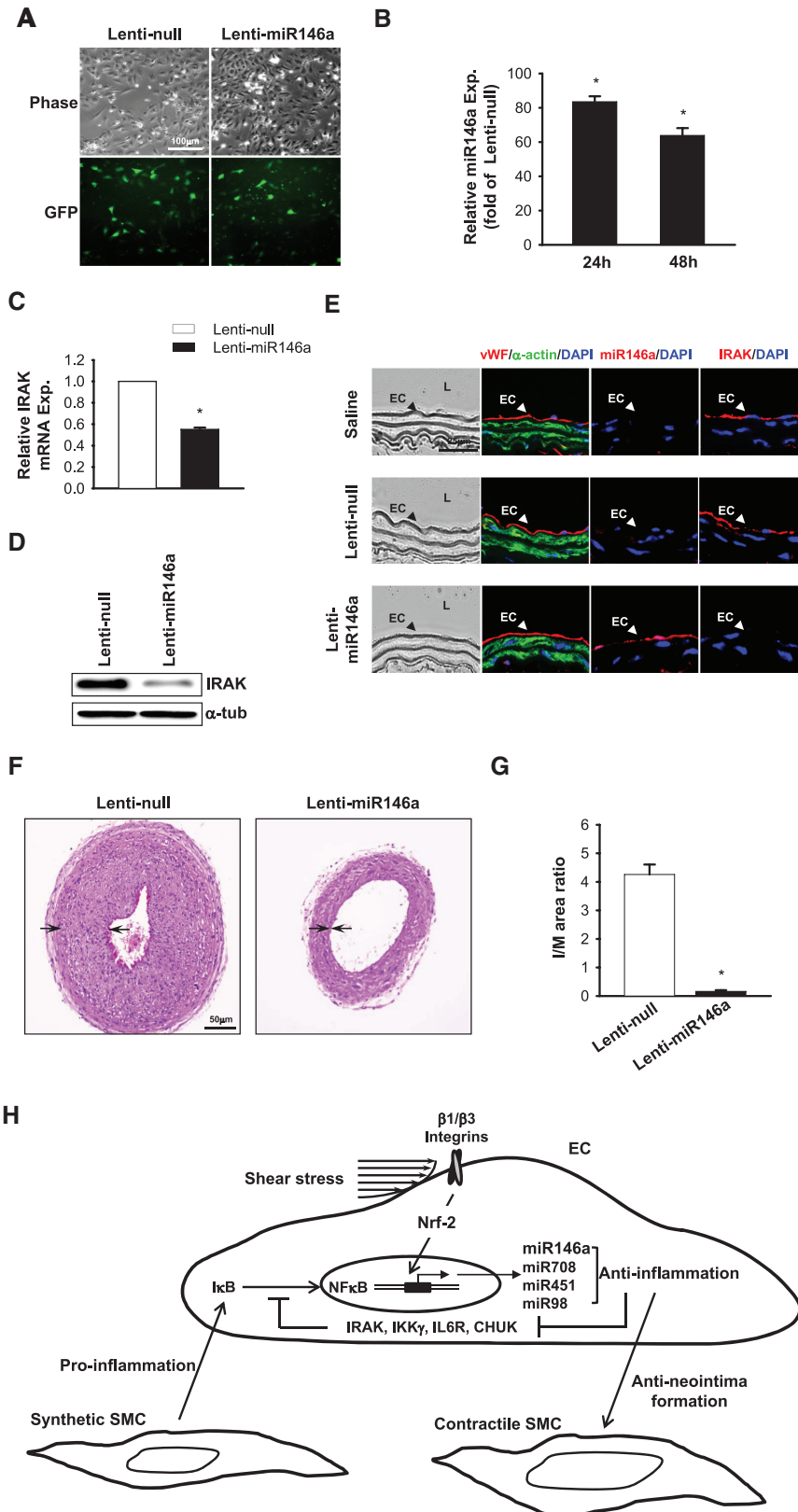


Figure 8. Lenti-miR-146a inhibits neointimal lesion formation in a mouse carotid artery ligation model. **A**, Cultured endothelial cells (ECs) were infected with Lenti-null or Lenti-miR-146a (5×10^8 TU/mL each) for 48 hours. **B**, MiR-146a expression was analyzed at 24 and 48 hours after infection. Interleukin-1 receptor–associated kinase (IRAK) mRNA (**C**) protein (**D**) expressions in infected ECs were determined. **E**, Serial cross-sections of the affected carotid arteries were stained for miR-146a and its direct target IRAK. L indicates lumen. Hematoxylin and eosin staining (**F**) and quantitative analysis (**G**) of neointimal lesions in the affected arteries. * $P < 0.05$ vs Lenti-null. Images shown in each examination are representative of 5 mice with similar results. **H**, A schematic diagram of the mechanisms underlying synthetic smooth muscle cells (sSMC)– and shear-modulations in EC miR expression. CHUK, conserved helix-loop-helix ubiquitous kinase; DAPI, 4',6-diamidino-2-phenylindole; GFP, green fluorescence protein; IKK- γ , inhibitor of NF- κ B kinase subunit- γ ; IL6R, interleukin-6 receptor; NF, nuclear factor; and vWF, von Willebrand factor.

flow. Thus, the compensatory responses for these 4 miRs are limited in capacity (duration) and they may fail over time, and need the rescue by laminar shear stress.

Our previous study showed that sSMCs release IL-1 β and IL-6 to induce E-selectin expression in adjacent ECs,² and that shear stress applied to ECs inhibits these sSMC-induced proinflammatory responses.^{2,3} This study advanced the new notion that miR-146a, miR-708, miR-451, and miR-98 are involved in regulating sSMC-induced EC inflammation under flow. MiR-146a and miR-98 were shown to be negative regulators against proinflammatory responses in ECs¹⁶ and other cell types.^{13,17} However, whether miR-708 and miR-451 can modulate cell inflammatory function has not been reported. Our study provides the first evidence to show that miR-708 and miR-451 exert anti-inflammatory effects on ECs by directly silencing IKK- γ and IL-6R genes, respectively, thus inhibiting EC NF- κ B activation, E-selectin expression, and monocyte adhesion. The notion that miR-451 plays anti-inflammatory roles in ECs was also substantiated by our recent findings that vascular cell adhesion molecule-1 is a direct target gene that can be silenced by miR-451 in ECs (Online Figure VII).

In this study, overexpressing miR-146a, miR-708, miR-451, and miR-98 in cocultured ECs inhibited sSMC-activation of EC p65 (Figure 3C). However, transfecting with anti-miRs had no effect on p65 signaling in cocultured ECs in comparison with scramble controls. Such nonsymmetrical effects of pre-miRs and anti-miRs on cell signaling have also been reported. For example, Huang et al¹⁸ showed that overexpressing miR-146a by its pre-miR decreases oscillatory pressure-activation of NF- κ B in human epithelial cells; however, inhibition of miR-146a by its anti-miR did not enhance NF- κ B activation. Inhibition of miR-222 in cultured SMCs increased their p57 expression, but overexpressing this miR had no effect on p57 mRNA level.¹⁹ These nonsymmetrical effects of pre- and anti-miRs might reflect the complication of regulatory pathways triggered by different physiological and pathophysiological microenvironments, which may not lead to opposite effects.

The putative promoter regions of miR-146a, miR-708, miR-451, and miR-98 contain ≥ 1 NF- κ B-binding sites. Our results on NF- κ B-regulation of sSMC-induction of these miRs in cocultured ECs suggest that the putative NF- κ B-binding elements in the promoter regions of these miRs are functional. NF- κ B was shown to regulate the expressions of miR-9, miR-155, and miR-146a, which in turn target the components of NF- κ B pathway to inhibit its activation by a negative feedback loop.^{13,20} Our study has discovered new miRs that serve as potential negative regulators of inflammation by inhibiting the NF- κ B pathway through negative feedback control.

Among the 4 miRs we studied, only miR-146a has been identified with its promoter sequences, which contain several Nrf-2-binding domains.¹³ An important new finding of this study is to identify Nrf-2 as a critical transcription factor for regulating miR-146a transcription in cocultured ECs in response to flow. Recent studies indicated that KLF-2 and Nrf-2 govern $\approx 70\%$ of shear-elicited gene sets in ECs.²¹ The involvement of KLF-2 in shear-modulation of miR-143/145

transcription in ECs has been reported.¹¹ However, whether Nrf-2 can modulate miR expression in ECs in response to shear has not been explored. Our study represents the first demonstration that Nrf-2 plays important roles in modulating shear-induction of miR transcription in cocultured ECs. Thus, our findings have closed a loop to indicate that both KLF-2 and Nrf-2 can modulate not only the shear-elicited genes but also the shear-elicited miRs in ECs.

ECs and SMCs may affect each other through secreted miRs. Hergenreider et al¹¹ showed that shear stress regulates EC expression of miR-143/145, which can be transferred by phospholipid vesicles to SMCs to modulate their phenotype. Our recent study showed that miR-126 can be secreted by ECs to affect sSMC proliferation, and that this EC secretion of miR-126 is inhibited by shear stress.¹² In this study, we found that pretreating EC/SMC coculture with GW4869, which is a neutral sphingomyelinase inhibitor that suppresses the secretion of exosomal miRs, had no effect on sSMC- and shear-modulations of EC miR-146a, miR-708, miR-451, and miR-98 (data not shown). Thus, sSMC- and shear-modulations of these EC miRs are not attributable to the secretion of exosomal miRs from sSMCs.

The nature of blood flow plays crucial roles in the pathogenesis of vascular disorders.¹ Our rat carotid artery constriction experiments demonstrated the importance of physiological levels of blood flow in the inductions of miR-146a, miR-708, miR-451, and miR-98 in ECs of neointimal lesions in injured carotid arteries. These 4 miRs did not show significant expression in ECs of control vessels, but they were highly expressed in injured carotid arteries, in which SMCs change their phenotype toward a synthetic state and migrate into the subendothelial layers to have close interactions with ECs. These high levels of miRs in ECs situated in close adjacency to sSMCs were reduced by partial ligation of the arteries, which created flow stagnation with more severe neointimal lesion formation than in the unligated arteries exposed to higher levels of flow. Thus, physiological levels of flow and shear stress induce miR-146a, miR-708, miR-451, and miR-98 expressions in ECs adjacent to sSMCs to exert anti-inflammatory effects to inhibit neointima formation of injured arteries.

Among the 4 miRs we studied, miR-146a has several unique features. First, miR-146a showed the largest increase in its expression in cocultured ECs in response to shear stress in comparison with other miRs on the arrays. Second, it exhibited remarkable induction in ECs of neointimal lesions in injured arteries. Third, its expression was more stable in cocultured ECs (Online Figure VIII). Thus, we performed miR-146a therapeutic experiments by using 2 animal models. In the rat carotid artery constriction model, Lenti-miR-146a was locally injected into the lumen of constricted carotid artery after balloon injury for 2 weeks, where the denudated EC layer had been recovered. In the mouse carotid artery ligation model, neointimal lesions were created in carotid artery by flow cessation, with the maintenance of an integral EC layer. Examinations on cross-sections of Lenti-miR-146a-affected arteries revealed that miR-146a induction in these arteries is more specific in the intact EC layer than the SMC regions (Figures 7E and 8E). This lentivirus-mediated overexpression

of mature miR-146a in intact EC layer inhibited neointimal lesion formation of these arteries, indicating that miR-146a is a potential hemodynamic-based therapeutic target for atherosclerosis and restenosis.

Our recent data indicate that changes in EC miR-146a expression may influence phenotype of sSMCs, which form neointima. Shear stress stimulation of cocultured ECs did not affect miR-146a expression in sSMCs in comparison with static control cells (Online Figure IXA). However, in concert with our previous findings,¹⁴ shear stress stimulation of cocultured ECs, which induced EC miR-146a expression, increased contractile marker smooth muscle α -actin expression and decreased retinoblastoma protein phosphorylation in sSMCs (Online Figure IXB). Transfecting cocultured ECs with pre-miR-146a under static condition can mimic shear stress effects to increase smooth muscle α -actin expression and decrease retinoblastoma phosphorylation in sSMCs. In contrast, transfecting cocultured ECs with anti-miR-146a abolished the shear stress effects on sSMCs. These results indicate that laminar shear stress applied to ECs may modulate sSMC phenotype toward a contractile state through EC miR-146a induction. This EC miR-146a-modulation of sSMC phenotype in response to flow may contribute to the therapeutic effect of miR-146a on arterial neointima formation under flow.

In addition to ECs, miR-146a may play protective roles against vascular inflammation through other cell types, such as white blood cells. MiR-146a was reported to inhibit lipopolysaccharides-induction of interferon- γ in lymphocytes.²² Genetic knockout of miR-146a has been shown to induce activation and maturation of monocytes and macrophages, resulting in several immune defects, such as myeloid malignancies.²³ These results indicate that miR-146a may play important roles in regulating innate immune and inflammatory responses through white blood cells. Although this study has clearly identified the action of miR-146 on ECs in its protective effect on neointima formation, the possible involvement of other types of cells in this protective effect warrants further investigations.

Several types of surgical interventions, such as percutaneous balloon angioplasty and stent placement, have been developed with the aim of restoring blood flow in vascular occlusive diseases.¹ These interventions, however, may themselves induce stagnant flow condition, thus leading to neointimal hyperplasia and atherosclerotic lesions.¹ Increase of blood flow is a critical strategy for preventing neointimal hyperplasia after percutaneous coronary intervention.^{1,24} Our findings that shear-induction of EC miR-146a not only can exert anti-inflammatory effects on ECs adjacent to sSMCs but also can modulate sSMC phenotype toward a contractile state, suggest the clinical perspective of miR-146a-related strategies and drugs for neointimal hyperplasia prevention after surgical interventions, such as percutaneous coronary intervention.

In summary, this study used a combination of in vitro EC/sSMC coculture flow system and in vivo experimental animal studies to demonstrate the anti-inflammatory effects of miR-146a, miR-708, miR-451, and miR-98 on ECs adjacent to sSMCs. These miRs become highly expressed in these ECs in response to atheroprotective shear stress. Nrf-2 regulates

shear-induction of miR-146a in these ECs at the transcriptional level. In addition, miR-146a plays a protective role against neointimal lesion formation in arteries. Our findings suggest miR-146a to be a valuable therapeutic miR for intervention against vascular occlusive diseases resulting from atherosclerosis and restenosis.

Acknowledgments

L.-J. Chen performed the research under the auspices of Graduate Program of Biotechnology in Medicine, National Tsing Hua University and National Health Research Institutes.

Sources of Funding

This work was supported by MOST-103-2321-B-400-001/MOST-103-2325-B-016-003 (to J.-J.C.), NSFC-81470590/BNSF-7152081 (to J.Z.), and HL-106579/HL-108735 (to S.C.).

Disclosures

None.

References

- Chiu JJ, Chien S. Effects of disturbed flow on vascular endothelium: pathophysiological basis and clinical perspectives. *Physiol Rev*. 2011;91:327–387. doi: 10.1152/physrev.00047.2009.
- Chiu JJ, Chen LJ, Lee CI, Lee PL, Lee DY, Tsai MC, Lin CW, Usami S, Chien S. Mechanisms of induction of endothelial cell E-selectin expression by smooth muscle cells and its inhibition by shear stress. *Blood*. 2007;110:519–528. doi: 10.1182/blood-2006-08-040097.
- Chiu JJ, Chen LJ, Chang SF, Lee PL, Lee CI, Tsai MC, Lee DY, Hsieh HP, Usami S, Chien S. Shear stress inhibits smooth muscle cell-induced inflammatory gene expression in endothelial cells: role of NF- κ B. *Arterioscler Thromb Vasc Biol*. 2005;25:963–969. doi: 10.1161/01.ATV.0000159703.43374.19.
- Krol J, Loedige I, Filipowicz W. The widespread regulation of microRNA biogenesis, function and decay. *Nat Rev Genet*. 2010;11:597–610. doi: 10.1038/nrg2843.
- Fang Y, Shi C, Manduchi E, Civelek M, Davies PF. MicroRNA-10a regulation of proinflammatory phenotype in athero-susceptible endothelium in vivo and in vitro. *Proc Natl Acad Sci U S A*. 2010;107:13450–13455. doi: 10.1073/pnas.1002120107.
- Fang Y, Davies PF. Site-specific microRNA-92a regulation of Kruppel-like factors 4 and 2 in atherosusceptible endothelium. *Arterioscler Thromb Vasc Biol*. 2012;32:979–987. doi: 10.1161/ATVBAHA.111.244053.
- Son DJ, Kumar S, Takabe W, Kim CW, Ni CW, Alberts-Grill N, Jang IH, Kim S, Kim W, Won Kang S, Baker AH, Woong Seo J, Ferrara KW, Jo H. The atypical mechanosensitive microRNA-712 derived from pre-ribosomal RNA induces endothelial inflammation and atherosclerosis. *Nat Commun*. 2013;4:3000. doi: 10.1038/ncomms4000.
- Qin X, Wang X, Wang Y, Tang Z, Cui Q, Xi J, Li YS, Chien S, Wang N. MicroRNA-19a mediates the suppressive effect of laminar flow on cyclin D1 expression in human umbilical vein endothelial cells. *Proc Natl Acad Sci U S A*. 2010;107:3240–3244. doi: 10.1073/pnas.0914882107.
- Wang KC, Garmire LX, Young A, Nguyen P, Trinh A, Subramaniam S, Wang N, Shyy JY, Li YS, Chien S. Role of microRNA-23b in flow-regulation of Rb phosphorylation and endothelial cell growth. *Proc Natl Acad Sci U S A*. 2010;107:3234–3239. doi: 10.1073/pnas.0914825107.
- Wu W, Xiao H, Laguna-Fernandez A, Villarreal G Jr, Wang KC, Geary GG, Zhang Y, Wang WC, Huang HD, Zhou J, Li YS, Chien S, Garcia-Cardena G, Shyy JY. Flow-dependent regulation of Kruppel-like factor 2 is mediated by microRNA-92a. *Circulation*. 2011;124:633–641. doi: 10.1161/CIRCULATIONAHA.110.005108.
- Hergenreider E, Heydt S, Tréguer K, Boettger T, Horrovoets AJ, Zeiher AM, Scheffer MP, Frangakis AS, Yin X, Mayr M, Braun T, Urbich C, Boon RA, Dimmeler S. Atheroprotective communication between endothelial cells and smooth muscle cells through miRNAs. *Nat Cell Biol*. 2012;14:249–256. doi: 10.1038/ncb2441.
- Zhou J, Li YS, Nguyen P, Wang KC, Weiss A, Kuo YC, Chiu JJ, Shyy JY, Chien S. Regulation of vascular smooth muscle cell turnover by endothelial cell-secreted microRNA-126: role of shear stress. *Circ Res*. 2013;113:40–51. doi: 10.1161/CIRCRESAHA.113.280883.

13. Taganov KD, Boldin MP, Chang KJ, Baltimore D. NF-kappaB-dependent induction of microRNA miR-146, an inhibitor targeted to signaling proteins of innate immune responses. *Proc Natl Acad Sci U S A*. 2006;103:12481–12486. doi: 10.1073/pnas.0605298103.
14. Malhotra D, Portales-Casamar E, Singh A, Srivastava S, Arenillas D, Happel C, Shyr C, Wakabayashi N, Kensler TW, Wasserman WW, Biswal S. Global mapping of binding sites for Nrf2 identifies novel targets in cell survival response through ChIP-Seq profiling and network analysis. *Nucleic Acids Res*. 2010;38:5718–5734. doi: 10.1093/nar/gkq212.
15. Zhou J, Wang KC, Wu W, Subramaniam S, Shyy JY, Chiu JJ, Li JY, Chien S. MicroRNA-21 targets peroxisome proliferators-activated receptor-alpha in an autoregulatory loop to modulate flow-induced endothelial inflammation. *Proc Natl Acad Sci U S A*. 2011;108:10355–10360. doi: 10.1073/pnas.1107052108.
16. Cheng HS, Sivachandran N, Lau A, Boudreau E, Zhao JL, Baltimore D, Delgado-Olguin P, Cybulsky MI, Fish JE. MicroRNA-146 represses endothelial activation by inhibiting pro-inflammatory pathways. *EMBO Mol Med*. 2013;5:949–966. doi: 10.1002/emmm.201202318.
17. Liu Y, Chen Q, Song Y, Lai L, Wang J, Yu H, Cao X, Wang Q. MicroRNA-98 negatively regulates IL-10 production and endotoxin tolerance in macrophages after LPS stimulation. *FEBS Lett*. 2011;585:1963–1968. doi: 10.1016/j.febslet.2011.05.029.
18. Huang Y, Crawford M, Higuera-Castro N, Nana-Sinkam P, Ghadiali SN. miR-146a regulates mechanotransduction and pressure-induced inflammation in small airway epithelium. *FASEB J*. 2012;26:3351–3364. doi: 10.1096/fj.11-199240.
19. Liu X, Cheng Y, Zhang S, Lin Y, Yang J, Zhang C. A necessary role of miR-221 and miR-222 in vascular smooth muscle cell proliferation and neointimal hyperplasia. *Circ Res*. 2009;104:476–487. doi: 10.1161/CIRCRESAHA.108.185363.
20. Leung AK, Sharp PA. MicroRNA functions in stress responses. *Mol Cell*. 2010;40:205–215. doi: 10.1016/j.molcel.2010.09.027.
21. Boon RA, Horrevoets AJ. Key transcriptional regulators of the vasoprotective effects of shear stress. *Hamostaseologie*. 2009;29:39–40, 41–43.
22. Dai R, Phillips RA, Zhang Y, Khan D, Crasta O, Ahmed SA. Suppression of LPS-induced Interferon-gamma and nitric oxide in splenic lymphocytes by select estrogen-regulated microRNAs: a novel mechanism of immune modulation. *Blood*. 2008;112:4591–4597. doi: 10.1182/blood-2008-04-152488.
23. Boldin MP, Taganov KD, Rao DS, Yang L, Zhao JL, Kalwani M, Garcia-Flores Y, Luong M, Devrekanli A, Xu J, Sun G, Tay J, Linsley PS, Baltimore D. miR-146a is a significant brake on autoimmunity, myeloproliferation, and cancer in mice. *J Exp Med*. 2011;208:1189–1201. doi: 10.1084/jem.20101823.
24. Koskinas KC, Chatzizisis YS, Antoniadis AP, Giannoglou GD. Role of endothelial shear stress in stent restenosis and thrombosis: pathophysiologic mechanisms and implications for clinical translation. *J Am Coll Cardiol*. 2012;59:1337–1349. doi: 10.1016/j.jacc.2011.10.903.

Novelty and Significance

What Is Known?

- In atherosclerotic lesions, synthetic smooth muscle cells (sSMCs) induce proinflammatory signaling and gene expression in endothelial cells (ECs) under conditions of reduced blood flow.
- Increases in blood flow and shear stress result in favorable signaling and gene modulations to mitigate the sSMC-induced EC inflammation.
- MicroRNAs (miRs) are noncoding small RNAs that play important roles in regulating EC function.

What New Information Does This Article Contribute?

- The levels of EC miR-146a, miR-708, miR-451, and miR-98 are elevated by atheroprotective shear stress in close adjacency to sSMCs to serve as negative regulators for sSMC-induced EC inflammation.
- Nuclear factor-E2-related factor-2 (Nrf-2) modulates the shear-induction of miR-146a in ECs in close adjacency to sSMCs at the transcriptional level.

- Overexpressing miR-146a inhibits neointima formation of arteries induced by injury or blood flow cessation.

A better understanding the molecular mechanisms by which sSMCs modulate EC gene expression and function and elucidation of the effects of shear stress on this modulation could provide new molecular targets for intervention against vascular disorders resulting from atherosclerosis and restenosis. We report that in ECs adjacent to sSMCs, miR-146a, miR-708, miR-451, and miR-98 become highly expressed in response to atheroprotective shear stress and play anti-inflammatory roles in vitro and in vivo. In addition, we found that Nuclear factor- κ B and Nrf-2 are involved in sSMC- and shear-modulations of these EC miR expressions at the transcriptional levels, respectively. MiR-146a serves as a valuable therapeutic miR for intervention against neointimal lesion formation that leads to atherosclerosis and restenosis.

SUPPLEMENTAL MATERIAL

ONLINE METHODS

Materials. Mouse monoclonal antibodies (mAb) against human p65, rabbit polyclonal antibodies (pAbs) against human p65 and Nrf-2, and anti-rabbit IgG were purchased from Santa Cruz Biotechnology (Santa Cruz, CA). Rabbit mAbs against human phospho-p65 and Ago2 were purchased from Cell Signaling Technology (Beverly, MA). Rabbit mAb against human phospho-I κ B was purchased from Epitomics (Burlingame, CA). Mouse mAb against human actin and rabbit mAb against human and rat vWF were purchased from Merck Millipore (Temecula, CA). Mouse mAbs against human LIBS-1 and LIBS-2 were purchased from Chemicon (Temecula, CA). Rabbit mAb against human Shc was purchased from Upstate (Lake Placid, NY). Mouse mAbs against human and rat α -tubulin and α -actin were purchased from Sigma (St. Louis, MO). Alexa Fluor-conjugated goat anti-rabbit IgG and Alexa Fluor-conjugated goat anti-mouse IgG secondary antibodies were purchased from Invitrogen (Carlsbad, CA). The wild-type (A547) and mutant (NF κ Bm2) of miR-146a promoter were purchased from Addgene (Cambridge, MA). Nrf-2-specific shRNA lentiviral particles were purchased from Santa Cruz Biotechnology. Anti-miR-146a and scramble control were chemically modified with cholesterol conjugated from a hydroxyprolinol-linked cholesterol solid support and 2'-OMe phosphoramidites (Ribobio). BAY117028 was purchased from Santa Cruz Biotechnology. Actinomycin D was purchased from Sigma. D,L-Sulforaphane was purchased from Merck Millipore. All other chemicals of reagent grade were purchased from Sigma, unless otherwise noted.

Cell culture. Human aortic ECs and SMCs were obtained commercially (Clonetics, Palo Alto, CA). ECs were grown in medium 199 (M199; Gibco, Grand Island, NY) supplemented with 20% fetal bovine serum (FBS; Gibco). SMCs were grown in F12K medium (Sigma) supplemented with 10% FBS. SMCs used in this study were in synthetic phenotype (sSMCs), as described^{1,2}. Cells between passages 4 and 7 were used in the experiments.

Co-culture flow system. EC/SMC co-culture was established by plating these two types of cells on the opposite sides of a 10- μ m-thick porous membrane, which was incorporated into a parallel-plate flow chamber, as described³. The wall shear stress applied to the ECs was 12 dynes/cm², as described³.

MiR array analysis. Total RNA from ECs was isolated using TRIzol (Invitrogen) according to the manufacturer's protocol. The expression of 380 mature human miRs in ECs was profiled using 384-well TaqMan human MicroRNA Assays (Applied Biosystems, Carlsbad,

CA). MiR expression data were normalized to RNU48.

Reverse transcriptase-polymerase chain reaction (RT-PCR). Five μg total RNA of ECs in co-culture was isolated by TRIzol (Invitrogen) according to the manufacturer's protocol, and then converted to cDNA using the Superscript II reverse transcriptase system and oligo-dT primers (Invotrogen). Briefly, total RNA (0.5-1 μg , in diethyl pyrocarbonate [DEPC] water) was incubated with 50 U/ μL Superscript II reverse transcriptase in a buffer containing 20 mmol Tris-HCl, 2.5 mmol MgCl_2 , 0.5 mmol deoxynucleoside triphosphate (dNTP) mix, 10 mmol/L dithiothreitol (DTT) and oligo-dT₁₂₋₁₈ (0.5 $\mu\text{g}/\text{mL}$) for 50 min at 42°C. Reactions were terminated with *Escherichia coli* RNase H (2 U/ μL) for 15 min at 70°C.

Quantitative real-time PCR (qPCR) for miR and mRNA expressions. For qPCR analysis of miR and mRNA expressions, cDNA from 1 μg total RNA was obtained by the SuperScript® II Reverse Transcriptase (Invitrogen). qPCR was performed on a LightCycler® 1.5 (Roche Diagnostics, Mannheim, Germany). MiR expression was validated by quantitative stem-loop PCR technology, as described^{4,5}. The use of target-specific reverse transcription primers and Universal Probe Library Probe #21 (Roche Diagnostic) allows the specific detection of mature miRs. A final volume of 20 μL consisted of 0.5 $\mu\text{mol}/\text{L}$ of each forward and reverse primer, 0.1 $\mu\text{mol}/\text{L}$ Probe #21, 1X LightCycler® TaqMan® Master (Roche Diagnostics), and 2.5 μL of cDNA. Amplification curves were generated with an initial denaturing step at 95°C for 10 min, followed by 45 cycles of 95°C for 5 sec, 60°C for 10 sec, and 70°C for 1 sec. MiR expression was normalized to the expression of the snU6. mRNA expression was also validated by qPCR technology. The LightCycler® TaqMan® Master (Roche Diagnostics) reaction mix was used for the Universal Probe Library assays. The amplification condition was initiated with denaturation at 95°C for 10 min, followed by 40-50 cycles of 95°C for 10 sec, 60°C for 20 sec, and 70°C for 5 sec. mRNA expression was normalized to the expression of β -actin and GAPDH. For primer sequences see Online Tables I and II.

MiR stability assay. To assess the *in vitro* stability of miRs in co-cultured ECs, total RNA was extracted at 6 h after addition of the RNA-polymerase inhibitor actinomycin D (10 $\mu\text{g}/\text{mL}$) to the culture medium from co-cultured ECs. A detailed procedure was previously described⁶.

Transfection. ECs were grown to 50-60% confluence, followed by transfection with 5-20 nmol/L pre-miRs, anti-miRs, or scramble controls (Ambion, Carlsbad, CA) by using Lipofectamine 2000 (Invitrogen), according to the manufacturer's protocol. For transfection with specific oligonucleotide siRNA, ECs were grown to 60-70 confluence and transfected

with the designed siRNAs at various concentrations (5, 10, 20, and 50 nmol/L) by using RNAiMAX (Invitrogen), according to the manufacturer's protocol. For *in vivo* transfection, 50 μ L of invivoFectamine 2.0 (Invitrogen) mixed with anti-miR-146a or scramble control (10 μ g each) were prepared, according to the manufacturer's protocol.

THP-1 Adhesion assay. ECs were transfected with specific pre-miRs or anti-miRs for 24 h, and then co-cultured with sSMCs. Monocytic THP-1 cells were obtained from American Type Culture Collection (Rockville, MD) and maintained in culture medium RPMI 1640 (Gibco) supplemented with 10% FBS. THP-1 cells were labeled with calcein acetoxymethyl ester (calcein-AM; Molecular Probes, Eugene, OR) at a concentration of 7.5 μ mol/L for 30 min to facilitate their visualization against the EC background. The labeled THP-1 cell suspension (5×10^5 cells/mL) was incubated with co-cultured ECs for 30 min. Non-adherent cells were removed by washing with cell-free buffer. The adherent THP-1 cells on the ECs were identified and counted in 20 or more randomly selected microscopic fields ($640 \mu\text{m} \times 480 \mu\text{m}$) under $\times 20$ objective (NA = 0.4, LD Achromplan, Zeiss), and the adhesion was expressed as cells/ mm^2 .

Western blot analysis. Co-cultured ECs on the transwell were collected by scraping and lysed with a buffer containing 1% NP-40, 0.5% sodium deoxycholate, 0.1% SDS, and a protease inhibitor mixture (PMSF, aprotinin, and sodium orthovanadate). The total cell lysate (10-50 μ g of protein) was separated by SDS-PAGE (10% running, 4% stacking) and transferred onto a polyvinylidene fluoride membrane (Immobilon P, 0.45- μ m pore size). The membrane was then incubated with the designated antibodies. Immunodetection was performed by using the Western-Light chemiluminescent detection system (Applied Biosystems).

Cytoplasmic and nuclear protein extraction. Cytoplasmic and nuclear proteins were extracted from ECs co-cultured with sSMCs response to shear stress by using ProteoJET™ Cytoplasmic and Nuclear Protein Extraction Kit (Thermo Scientific) according to the manufacturer's protocol. ECs co-cultured with sSMCs were collected by scraping and lysed with cell lysis buffer. Cell lysate was separated into cytoplasmic nuclear fractions by centrifugation at $500 \times g$ for 7 min at 4°C , and the supernatant (cytoplasmic protein extract) was carefully removed into a new tube. The nuclei were washed by nuclei washing buffer and the nuclear protein was lysed by nuclei lysis reagent for 15min at 4°C for 15mins. Nuclear lysate was purified by centrifugation at $20,000 \times g$ for 5 min at 4°C . The supernatant (nuclear protein extract) was transferred to a new tube for use.

Electrophoretic mobility shift assay (EMSA). ECs in co-culture were collected by scraping

in PBS. After centrifugation at 2000 rpm, the cell pellets were resuspended in cold buffer A (containing, in mmol/L, KCl 10, ethylenediamine tetraacetate [EDTA] 0.1, dithiothreitol [DTT] 1, and phenyl methylsulfonyl fluoride [PMSF] 1) for 15 min. The cells were lysed by adding 10% NP-40 and then centrifuged at 6000 rpm to obtain pellets of nuclei. The nuclear pellets were resuspended in cold buffer B (containing, in mmol/L, 4-(2-hydroxyethyl)-1-piperazine-ethane-sulfonic acid [HEPES] 20, EDTA 1, DTT 1, PMSF 1, and NaCl 400), vigorously agitated, and then centrifuged. The supernatant containing the nuclear proteins was used for the EMSA or stored at -70°C until used. NF-κB (5'-AGTTGAGGGGACTTCCAGGC-3', Promega, Fitchburg, WI) and ARE (5'-CTACGATTCTGCTTAGTCATTGTCTTCC-3') consensus oligonucleotides were measured for NF-κB and ARE binding activities, respectively. The oligonucleotides were end-labeled with [γ -³²P] ATP. The extracted nuclear proteins (5 μg) were incubated with 0.1 ng ³²P-labeled DNA for 15 min at room temperature in 25 μL binding buffer containing 1 μg poly(dI-dC). In the antibody supershift assay, antibodies to NF-κB subunits p65 and Nrf-2 (1 μg each) were incubated with the mixture for 10 min at room temperature, followed by the addition of the labeled probe. The mixtures were electrophoresed on 6% nondenaturing polyacrylamide gels. The gels were dried and imaged by autoradiography.

Chromatin immunoprecipitation (ChIP) assay. ChIP assay was performed according to the manufacturer's protocol (EZ-ChIPTM; Merck Millipore). In brief, ECs were treated with 1% formaldehyde and subjected to sonication in SDS lysis buffer containing a protease inhibitor cocktail. Immunoprecipitation was performed with either anti-p65 or anti-Nrf-2 antibody (1 μg/100 μL; Santa Cruz). Input and immunoprecipitated chromatin were incubated at 65°C overnight to reverse the crosslinks. DNA was eluted and PCR was performed with the p65 (sense: 5'-GAAGCTGACACTGCCAGGCT-3'; antisense: 5'-TTTCCACACCCTGCACGCTAA-3') and Nrf-2 (sense: 5'-GCGCCTGACCAGAACTTCCT-3'; antisense: 5'-TCATGCGTGCAGGGTCT-3') primers. All primers used in this study are listed in Online Tables I and II.

MicroRNA target prediction. Target genes for miR-146a, -708, -451 and -98 were predicted using the free software PicTar (<http://pictar.mdc-berlin.de/>), microRNA.org (<http://www.microrna.org/microrna/home.do>) and TargetScan 4.2 (<http://www.targetscan.org/>) with the cutoff set at *P* value less than 0.05.

Ago2 complex immunoprecipitation. ECs were collected by scraping and lysed, as described³. Cell lysates were centrifuged at 13000 rpm for 10 min. An anti-Ago2 antibody (1 μg/100 μL; Cell Signaling) was added and incubated with rotation at 4°C overnight, and the immune complexes were then isolated with protein A/G Sepharose beads. RNA was extracted with the TRIzol reagent, and the purified RNA was analyzed by qPCR.

3'-UTR luciferase reporter assays. To produce 3'-UTR luciferase reporter constructs, synthetic oligonucleotide binding sequence or a mutated sequence fragments (~40 bp) of 3'-UTRs of IRAK1, IKK γ , IL-6R, CHUK, and VCAM-1 genes were cloned into the downstream of CMV-driven firefly luciferase cassette in pMIR-REPORT vector (Ambion) according to the manufacturer's protocol. HEK293 cells were grown in 6-well plates until 60-70% confluence, and 1.5 μ g luciferase plasmid was co-transfected with 0.5 μ g β -galactosidases. In some experiments, pre-miRs, anti-miRs, or scramble controls were co-transfected into the cells using Lipofectamine 2000 (Invitrogen). The luciferase activity was assessed after 48 h with the Dual-Luciferase(R) Reporter 1000 Assay System (Promega).

Animal model. Adult Two animal models were used in this study. Carotid artery balloon injury was performed in male Sprague-Dawley rats (350-500 g), and carotid artery ligation was performed in female FVB/NJ mice (12 weeks of age), as described⁷. All animals were euthanized by intoxication with 100% carbon dioxide. Carotid arteries were harvested, post-fixed, paraffin-embedded, and sectioned. All animals and experiments were maintained and performed according to the guidelines of the Animal Research Committee of National Health Research Institutes.

MiR *in situ* hybridization. A modified *in situ* hybridization protocol⁸ was used in this study. Briefly, cross sections of carotid arteries were incubated in 20 nmol/L of 5'-DIG-labeled locked-nucleic acid probes (LNA miRCURY probe, Exiqon) at an optimal temperature followed by incubation with HRP-conjugated anti-DIG antibody (Roche Applied Science) and signal amplification with TMR-tyramide (PerkinElmer). The slides were mounted, and images were acquired and analyzed using a Zeiss fluorescence microscope with Axiovision image analysis software.

Immunohistochemistry. Immunohistochemistry was performed on sections of paraffin-embedded rat carotid artery using EC and SMC specific markers (i.e., vWF and SM α -actin, respectively). The sections were de-waxed in xylene, rehydrated in descending grades of alcohol, and permeabilized by incubating for 10 min in sodium citrate for 10 min at 95°C. Sections were cooled down to room temperature and blocked with blocking reagent (Merck Millipore) for 30 min, and then incubated with primary antibodies overnight at 4°C. Alexa Fluor 594-conjugated goat anti-rabbit IgG (1:1000; Invitrogen) and Alexa Fluor 488-conjugated goat anti-mouse IgG (1:1000; Invitrogen) secondary antibodies in blocking reagent were incubated for 1 h at room temperature. Nuclei were co-stained by DAPI (Invitrogen) with PBS for 10 min. The sections were spin-dried and mounted with ProLong Gold (Invitrogen) on glass coverslips. Images were acquired and analyzed using a Zeiss fluorescence

microscope with Axiovision image analysis software.

Rat carotid artery balloon injury model. Carotid artery balloon injury model was created, as described⁹. In brief, rats were anesthetized under appropriate isoflurane concentration throughout the surgical procedure. The left common carotid artery (LCA) was exposed through a midline cervical incision. Temporarily ligations were performed on the proximal of LCA and distal of both external and internal carotid artery, and an arteriotomy site was then created on the external carotid artery for the insertion of 2F Fogarty embolectomy catheter (Edwards Lifesciences, Irvine, CA). Inserted catheter was slowly inflated to a pre-determined volume (0.02 mL) with saline and rotated within the common carotid artery. Blood flow was restored and wound was closed with 6-0 suture. In addition to studies under physiological levels of flow, the affected arteries were subjected to a partial ligation ($\approx 60\%$ constriction in diameter) at the proximal edge to create the stagnation flow condition^{10, 11}. Rats were left undisturbed for 4 weeks before scarification. Animals were euthanized by intoxication with 100% carbon dioxide. Carotid arteries were then harvested and post-fixed. Fixed carotid arteries were paraffin-embedded and sectioned. Sections received immunofluorescence, H&E and fluorescence *in situ* hybridization staining.

Delivery of lentiviral shRNA, miR, and chemically-modified miRs *in vivo*. For local delivery of lentiviral shRNA, miR and chemically-modified anti-miR-146a, secondary arteriotomy was performed on the external left common carotid artery (proximal to the first arteriotomy site) using microdissecting scissors two weeks after balloon injury. The blood flow was temporarily interrupted by ligation of the proximal LCA and distal of both external and internal carotid artery using 6-0 nylon suture. A 2F uncoated polyurethane catheter (Solomon scientific, San Antonio, TX) was introduced through the incision on the left external common carotid artery toward the balloon injured site. The catheter was then temporarily secured with a loose suture to prevent displacement during the local delivery. Fifty μL of lentiviral control, Nrf-2-specific shRNA, and Lenti-miR-146a (1×10^6 TU/mL each), chemically-modified scramble control and anti-miR-146a (10 μg each) were respectively infused into the local balloon injured site using gastight microsyringes (Hamilton, Reno, NV), followed by incubation for 30 min. The left external common carotid artery was ligated after the withdrawal of the solution, and blood flow was restored. Rats were left undisturbed for 4 weeks after balloon injury. Animals were euthanized by intoxication with 100% carbon dioxide. Carotid arteries were then harvested and post-fixed. Fixed carotid arteries were paraffin-embedded and sectioned. Sections received immunofluorescence, H&E and *in situ* hybridization staining.

Mouse vascular injury and lentiviral transfection. 12-weeks-old FVB/NJ mice were

anesthetized under appropriate isoflurane concentration. The left carotid artery was exposed and ligated proximate to carotid bifurcation, as described⁷. 5×10^7 TU lentiviral-null and lentiviral-miR-146a were injected from tail vein for every week. Mice were sacrificed at 4 weeks post-surgery. Mice were euthanized by intoxication with 100% carbon dioxide. Carotid and thoracic arteries were then harvested and fixed. Fixed arteries were either freshly *en-face* stained or paraffin embedded for sectioning. Sections received immunofluorescence, H&E and fluorescence *in situ* hybridization staining.

En face preparation and staining. Mice were euthanized by intoxication with 100% carbon dioxide. The carotid and thoracic arteries were perfusion-fixed with 100 mL of lukewarm-saline. The carotid and thoracic arteries were carefully dissected, removed adventitia and post fixed in fixative solution for overnight. The arteries were longitudinally dissected with microdissecting scissors and pinned flatly on a black wax dissection pan. For *en face in situ hybridization*, the luminal surfaces of the arteries were incubated with 0.5% Triton X-100 for 10 min, and then pre-hybridized in hybridization buffer for 30 min with temperature below the predicted T_m value of the LNA probe. The 5'-DIG-labeled LNA probes were then added to the sections at a 20 nmol/L concentration and incubated for 1 h at same temperature as pre-hybridization. vWF (1:100; Merck Millipore) was used for primary antibody and incubated in 10% FBS at 4°C for overnight. The luminal surfaces of the arteries were incubated with HRP-conjugated anti-DIG antibody (Roche Applied Science) for 30 min at room temperature, followed by TMR-tyramide signal amplification (PerkinElmer) for 10 min at room temperature in the dark. Alexa Fluor 488-conjugated goat anti-rabbit IgG (1:300; Invitrogen) was added at room temperature for 1 h. Nuclei were counterstained by DAPI with PBS for 10 min, rinsed three times in PBS, mounted with ProLong Gold (Invitrogen) on glass coverslips, and photographed with a Leica TCS SP5 confocal microscope. For GFP *en-face* staining, the luminal surfaces of the arteries were immediately blocked with 10% FBS for 1 h, followed by incubation with the designated primary antibodies GFP (1:500-1000; GeneTex, Irvine, CA) and vWF (1:100; Invitrogen) at 4°C overnight. Alexa Fluor 594-conjugated anti-rabbit IgG (1:300; Invitrogen) and Alexa Fluor 488-conjugated anti-goat IgG (1:300; Invitrogen) were used as secondary antibodies.

Ultrasound measurement. The ultrasound measurements were performed by using the iE33 ultrasound imaging system (Philips Medical Systems) equipped with a 7-15 MHz linear array transducer (L-15-7io), as described¹⁰. After balloon injury for 4 weeks, rats were anesthetized with chloral hydrate and placed in a supine position. The neck area was shaved and applied ultrasound gel for ultrasonic procedure. Levels of anesthesia, heart rate and respiratory pattern were continuously monitored. 2D color Doppler mode was used to identify the location and image of LCA. Pulse wave Doppler mode was used to measure the flow velocity at the distal

of LCA near the carotid bifurcation. Images were digitally stored for online measurement and later offline analysis.

Morphometric analysis for neointimal formation. Morphometric analysis *via* computerized image analysis software (Imaged J) was performed on the sections stained with H&E. Six sections (5 μm) at equally site intervals of injured carotid arteries were used. The neointima formation and vascular remodel were identified as neointima, medial, and luminal regions. The average of the six sections was used for one animal. The neointima formation was assessed as ratios of neointimal to medial thickness from 5 blocks of injured carotid arteries.

Statistical analysis. Results are expressed as mean \pm SEM. Statistical analysis was performed by using an independent Student t-test for two groups of data and analysis of variance (ANOVA) followed by Scheffe's test for multiple comparisons. A *P* value less than 0.05 was considered significant.

ONLINE RESULTS

Integrins regulate shear-inductions of miR-146a, -708, -451, and -98 in co-cultured ECs.

To investigate whether integrins regulate shear-inductions of miR-146a, -708, -451, and -98 in co-cultured ECs, ECs were pre-treated with poly-L-lysine (100 $\mu\text{g}/\text{mL}$; Online Figure IVA) and RGDS (500 $\mu\text{g}/\text{mL}$; Online Figure IVB) for 2 h to block the interactions between integrin and extracellular matrix (ECM) proteins, and then co-cultured with sSMCs under static conditions or in response to flow for 24 h. The poly-L-lysine and RGDS pre-treatments inhibited the shear-inductions of miR-146a, -708, -451, and -98 in co-cultured ECs, but they had no effect on sSMC-modulations of these miRs. Application of shear stress to ECs co-cultured with sSMCs induced sustained activations of β_1 and β_3 integrins and Shc over the 1-h period tested (Online Figure IVC). As controls, co-culturing ECs with sSMCs under static condition did not activate β_1 and β_3 integrins, or Shc, in ECs (data not shown). Transfecting ECs with β_1 - and β_3 -integrin-specific siRNAs (20 nmol/L each), which reduced the expression of the respective integrins by $\approx 70\%$ (compared with control siRNA), inhibited the shear-induction of these four miRs in co-cultured ECs (Online Figure IVD). Pre-treating ECs with poly-L-lysine (Online Figure IVE) and transfecting with β_1 - or β_3 -integrin-specific siRNAs (Online Figure IVF) inhibited the shear-induced translocation of Nrf-2 and its binding to the promoter region of miR-146a in the nucleus of co-cultured ECs, indicating that shear-activation of Nrf-2 in co-cultured ECs is modulated by β_1 and β_3 integrins.

ONLINE REFERENCES

1. Chen CN, Li YS, Yeh YT, Lee PL, Usami S, Chien S, Chiu JJ. Synergistic roles of platelet-derived growth factor-bb and interleukin-1beta in phenotypic modulation of human aortic smooth muscle cells. *Proc Natl Acad Sci U S A*. 2006;103:2665-2670
2. Tsai MC, Chen L, Zhou J, Tang Z, Hsu TF, Wang Y, Shih YT, Peng HH, Wang N, Guan Y, Chien S, Chiu JJ. Shear stress induces synthetic-to-contractile phenotypic modulation in smooth muscle cells via peroxisome proliferator-activated receptor alpha/delta activations by prostacyclin released by sheared endothelial cells. *Circ Res*. 2009;105:471-480
3. Chiu JJ, Chen LJ, Lee PL, Lee CI, Lo LW, Usami S, Chien S. Shear stress inhibits adhesion molecule expression in vascular endothelial cells induced by coculture with smooth muscle cells. *Blood*. 2003;101:2667-2674
4. Wu RM WM, Thrush A, Walton EF, Varkonyi-Gasic E Real time quantification of plant mirna using universal probelibrary technology. *Biochemica*. 2007;2:12-15
5. Leucht C, Bally-Cuif L. The universal probelibrary- a versatile tool for quantitative expression analysis in the zebrafish. *Biochemica*. 2007;2:16-18
6. Chiu JJ, Chen LJ, Chang SF, Lee PL, Lee CI, Tsai MC, Lee DY, Hsieh HP, Usami S, Chien S. Shear stress inhibits smooth muscle cell-induced inflammatory gene expression in endothelial cells: Role of nf-kappab. *Atertio Thromb Vasc Biol*. 2005;25:963-969
7. Kumar A, Lindner V. Remodeling with neointima formation in the mouse carotid artery after cessation of blood flow. *Atertio Thromb Vasc Biol*. 1997;17:2238-2244
8. Silaharoglu AN, Nolting D, Dyrskjot L, Berezikov E, Moller M, Tommerup N, Kauppinen S. Detection of micornas in frozen tissue sections by fluorescence in situ hybridization using locked nucleic acid probes and tyramide signal amplification. *Nat Protoc*. 2007;2:2520-2528
9. Tulis DA. Rat carotid artery balloon injury model. *Methods Mol Med*. 2007;139:1-30
10. Zhou J, Lee PL, Tsai CS, Lee CI, Yang TL, Chuang HS, Lin WW, Lin TE, Lim SH, Wei SY, Chen YL, Chien S, Chiu JJ. Force-specific activation of smad1/5 regulates vascular endothelial cell cycle progression in response to disturbed flow. *Proc Natl Acad Sci U S A*. 2012;109:7770-7775
11. Kohler TR, Jawien A. Flow affects development of intimal hyperplasia after arterial injury in rats. *Atertio Thromb Vasc Biol*. 1992;12:963-971

ONLINE TABLE LEGENDS

Online Table I. A list of primers used for qPCR analysis of miR expression.

Online Table II. A list of primers used for qPCR analysis of gene expression.

Online Table III. Analysis of the expression of miRs on the miR array. Data are mean \pm SEM from three independent experiments. N/A: not available: data of at least one experiment cannot be detected. *: a mean co-culture/monoculture ratio ≥ 2.0 and $P \leq 0.05$. **: a mean co-culture/monoculture ratio ≤ 0.5 and $P \leq 0.05$.

ONLINE FIGURE LEGENDS

Online Figure I. Schematic diagram of sequence alignments of miR-146a, -708, -451 and -98 and their target sites in 3'-UTRs of IRAK, IKK γ , IL-6R and CHUK, respectively. Filled bars correspond to reporter constructs with wild-type miRs targeting sites, and open bars correspond to constructs with 4-5 nucleotide substitution disrupting the base-pair with the seed region of the miRs.

Online Figure II. The effects of anti-miRs on I κ B phosphorylation in co-cultured ECs. ECs were transfected with the indicated concentrations of anti-miR-146a, -708, -451, and -98, or a scramble control for 24 h. These transfected ECs were kept alone as monocultured controls or co-cultured with sSMCs. The phosphorylation of I κ B was determined by Western blot. Results are representative of triplicate experiments with similar results.

Online Figure III. Schematic diagram of pri-miR-146a promoter assay. Sequence analysis of the pri-miR-146a promoter was performed by the ConSite on-line program. Four putative Nrf-2 binding elements in the promoter region of pri-miR-146a are shown.

Online Figure IV. Shear-inductions of miR-146a, -708, -451 and -98 in co-cultured ECs are regulated by β_1 and β_3 integrins. ECs were pre-treated with fibronectin (FN) and poly-L-lysine (PL) (A), RGE and RGD peptides (B), and then kept as controls or co-cultured with sSMCs under static conditions for 24 h. In parallel experiments, the co-cultured ECs were subjected to shear stress for 24 h. (C) ECs were cultured alone or co-cultured with sSMCs for 24 h, followed by exposure to shear stress for 5, 15, 30 or 60 min. The expressions of active β_1 (LIBS1) and β_3 (LIBS2) integrins and the phosphorylation of Shc were determined by Western blot. (D) ECs were transfected with β_1 - and β_3 -integrin-specific siRNAs (si β_1 and si β_3) or control siRNA (siCL), and then kept as controls or co-cultured with sSMCs under static conditions. In parallel experiments, the co-cultured ECs were subjected to shear stress for 24 h. Before co-culture with sSMCs and exposure to shear stress, ECs were pre-treated with FN or PL (E), or transfected with si β_1 , si β_3 , or siCL (F) The accumulation of Nrf-2 in the EC nuclei and the binding of Nrf-2 to the promoter region of miR-146a were determined by Western blot and ChIP assay, respectively. * P <0.05 vs. CL EC/SMC. # P <0.05 vs. FN, RGE, or siCL. Data in A, B, and D are means \pm SEM from three independent experiments. Results in C, E, and F are representative of triplicate experiments with similar results.

Online Figure V. MiR-146a, -708, -451, and -98 are highly expressed in the endothelial layer of injured arteries under physiological levels of flow. (A) Serial cross-sections of the

affected carotid arteries from injury/unconstructed and injury/constricted models were stained for miR-146a, -708, -451, and -98. ECs and SMCs were stained for vWF and SM α -actin, respectively, and were counterstained with DAPI. L, lumen. **(B)** Quantitative analysis of fluorescence intensity of these four miRs in the affected carotid arteries from different experimental models. Data are means \pm SEM for the EC layer from five independent experiments. * P <0.05 vs. control vessels. Images shown in each examination are representative of five rats with similar results.

Online Figure VI. *En face in situ* hybridization of miR-146a expression in the mouse carotid artery. FVB/NJ mice were received saline, Lenti-null, or Lenti-miR-146a every week by tail vein injection for 4 weeks. **(A)** *En face* immunofluorescence staining of GFP expression in the luminal surfaces of mouse carotid arteries. **(B)** *En face in situ* hybridization on the miR-146a expression in the luminal surfaces of mouse carotid arteries. ECs and SMCs were stained for vWF and SM α -actin, respectively. All staining sections were counterstained with DAPI. Scramble: negative control, U6: positive control. L, lumen. **(C)** Quantitative analysis of scramble, U6 and miR-146a fluorescence intensity in the affected carotid arteries from different experimental models. Data are means \pm SEM for the EC layer from five independent experiments. * P <0.05 vs. saline treatment. Images shown in each examination are representative of five mice with similar results.

Online Figure VII. VCAM-1 is a direct target gene of miR-451. **(A)** Schematic diagram of sequence alignment of miR-451 and its target sites in the 3'-UTR of VCAM-1. Filled bars correspond to reporter constructs with wild-type miR-451 targeting sites, and open bars correspond to constructs with a 4 nucleotide substitution disrupting the base-pair with the seed region of miR-451. **(B)** Reporter constructs containing wild-type (Wt) and mutant (Mut) of putative miR-451 target sites of VCAM-1 gene were co-transfected with pre-miR-451 or a scramble control (SC) into HEK293 cells for 24 h, and their luciferase activities were analyzed. **(C)** ECs were transfected with pre-miR-451 or a scramble control for 24 h, and the Ago2 immunoprecipitation assay was performed. Expression levels of VCAM-1 gene were detected by qPCR and normalized to the level of Ago2 protein. Data are mean \pm SEM from three independent experiments. * P <0.05 vs. empty vector. # P <0.05 vs. scramble control.

Online Figure VIII. Differential stabilities of the sSMC-induced EC expressions of miR-146a, -708, -451, and -98. ECs were kept alone as monocultured controls or co-cultured with sSMCs for the optimal period of time to increase the expression of the indicated miRs. Actinomycin D (10 μ g/mL) was then added into the medium for 6 h. The expression of indicated miRs was quantified by qPCR. Data are mean \pm SEM from three independent experiments. * P <0.05 vs. CL EC/SMC.

Online Figure IX. EC miR-146a affects SMC phenotype. (A) sSMCs were cultured alone (SMC/NC) or co-cultured with ECs (EC/SMC) under static conditions (CL). In parallel experiments, the co-cultured ECs were subjected to shear stress at 12 dynes/cm² for 24 h (SS). The expression of the miR-146a in sSMCs was examined by qPCR. (B) ECs were transfected with pre-miR-146a, anti-miR-146a, or a scramble control (SC) (20 nmol/L each) for 24 h, and then were cultured alone or co-cultured with sSMCs under static conditions or in response to shear stress. The phosphorylation of Rb and expression of SM α -actin in co-cultured sSMCs were analyzed by Western blot. Data are means \pm SEM from three independent experiments. * $P < 0.05$ vs. CL EC/SMC+SC.

Online Table I . A list of primers used for qPCR analysis of miR expression.

miR names		Sequence(5'-3')
miR-146a	RT stem-loop	GTTGGCTCTGGTGCAGGGTCCGAGGTATTCGCACCAGAGCCAACAACCCA
	forward	GCGCTGAGAACTGAATTCCA
miR-708	RT stem-loop	GTTGGCTCTGGTGCAGGGTCCGAGGTATTCGCACCAGAGCCAACCCCAGC
	forward	CGCGAAGGAGCTTACAATCTA
miR-451	RT stem-loop	GTTGGCTCTGGTGCAGGGTCCGAGGTATTCGCACCAGAGCCAACAACCTCA
	forward	CGCGAAACCGTTACCATTAC
miR-98	RT stem-loop	GTTGGCTCTGGTGCAGGGTCCGAGGTATTCGCACCAGAGCCAACAACAAT
	forward	GCGCTGAGGTAGTAAGTTG
miR-30b	RT stem-loop	GTTGGCTCTGGTGCAGGGTCCGAGGTATTCGCACCAGAGCCAACAGCTGA
	forward	GCGCTGTAAACATCCTACAC
miR-30c	RT stem-loop	GTTGGCTCTGGTGCAGGGTCCGAGGTATTCGCACCAGAGCCAACGCTGAG
	forward	GCGCTGTAAACATCCTACAC
miR-885	RT stem-loop	GTTGGCTCTGGTGCAGGGTCCGAGGTATTCGCACCAGAGCCAACAGAGGC
	forward	GCGCTCCATTACACTACCCT
miR-149	RT stem-loop	GTTGGCTCTGGTGCAGGGTCCGAGGTATTCGCACCAGAGCCAACGGGAGT
	forward	CCCGTCTGGCTCCGTGTCTT
miR-654-3p	RT stem-loop	GTTGGCTCTGGTGCAGGGTCCGAGGTATTCGCACCAGAGCCAACAAGGTG
	forward	GGGCTATGTCTGCTGACCAT
Universal	reverse	GTGCAGGGTCCGAGGT

Online Table II. A list of primers used for qPCR analysis of gene expression.

Gene names	Sequence(5'–3') forward	Sequence(5'–3') reverse
GAPDH	AGCCACATCGCTCAGACAC	GCCCAATACGACCAAATCC
IRAK	GAGACCTTGGCTGGTCAGAG	GTGCTTCTCAAAGCCACTCC
IKK γ	CGGAAATGCCTCACATATAGTTT	CCCAGTACGTCCTGATCTGC
IL6R	GTACCACTGCCCACATTCCT	TTCCACGTCTTCTTGAACCTC
CHUK	TGCAGTAACCCCTCAGACATC	TCTATCATTTGTGCTGAAGTCTCC
VCAM-1	TGGACATAAGAACTGGAAAAGG	CCACTCATCTCGATTTCTGGA
E-selectin	ACCAGCCCAGGTTGAATG	GGTTGGACAAGGCTGTGC
Nrf-2	GCGCCTGACCAGAACTTCCT	TCATGCGTG CAGGGTCT
P65	GAAGCTGACACTGCCAGGCT	TTCCACACCCTGCACGCT AA
pri-miR-146a	CAGTGGCTGAATTGGAAATG	AAAGACCCCTCCTTGCAGTC

Online Table III. Analysis of the expression of miRs on the miR array.

miR names	CL EC/SMC	<i>P</i> -value	SS EC/SMC	<i>P</i> -value
	CL EC/NC		CL EC/SMC	
hsa-miR-708	*46.74±15.27	<0.05	0.70±0.42	0.48
hsa-miR-146a	*15.51±4.31	<0.05	0.89±0.18	0.57
hsa-miR-98	**0.50±0.03	<0.05	2.34±0.13	<0.05
hsa-miR-30b	**0.45±0.07	<0.05	1.41±0.14	<0.05
hsa-miR-30c	**0.42±0.09	<0.05	1.13±0.10	0.25
hsa-miR-885	**0.23±0.09	<0.05	0.99±0.09	0.89
hsa-miR-149	**0.21±0.03	<0.05	1.28±0.41	0.53
hsa-miR-654-3p	**0.15±0.07	<0.05	1.92±1.11	0.46
hsa-miR-451	**0.07±0.04	<0.05	8.76±2.23	<0.05
hsa-miR-582-5p	16.22±8.63	0.15	8.90±7.25	0.34
hsa-miR-450a	13.34±12.79	0.39	2.02±1.50	0.53
hsa-miR-135b	11.34±10.84	0.39	7.58±7.57	0.43
hsa-miR-137	10.88±7.78	0.27	0.76±0.31	0.48
hsa-miR-184	9.14±6.46	0.28	0.07±0.05	<0.05
hsa-miR-199b	8.64±5.69	0.25	3.79±3.67	0.49
hsa-miR-520g	8.40±3.40	0.43	0.05±0.05	<0.05
hsa-miR-200a	7.80±4.91	0.24	2.64±1.54	0.35
hsa-miR-508	7.41±7.36	0.43	0.35±0.33	0.12
hsa-miR-146b	7.11±7.11	0.44	0.02±0.02	<0.05

hsa-miR-369-5p	6.72±6.01	0.40	1.16±0.58	0.79
hsa-miR-518e	6.54±3.51	0.19	0.53±0.09	<0.05
hsa-miR-597	6.51±6.06	0.41	2.29±0.79	0.18
hsa-miR-133a	6.22±5.36	0.38	0.15±0.08	<0.05
hsa-miR-9	6.19±5.17	0.37	13.67±12.24	0.36
hsa-miR-381	6.10±3.23	0.19	0.45±0.34	0.18
hsa-miR-141	5.91±5.41	0.42	1.34±1.31	0.81
hsa-miR-138	5.46±3.81	0.31	9.01±8.49	0.40
hsa-miR-202	5.27±5.14	0.45	7.92±6.98	0.38
hsa-miR-503	4.01±3.24	0.40	5.67±4.22	0.33
hsa-miR-346	3.45±1.42	0.16	0.96±0.73	0.96
hsa-miR-380	3.34±3.34	0.52	0.03±0.03	<0.05
hsa-miR-330-5p	3.33±3.05	0.49	0.08±0.04	<0.05
hsa-miR-502-5p	3.30±1.65	0.24	5.66±4.91	0.40
hsa-miR-429	3.21±2.71	0.46	4.02±2.13	0.23
hsa-miR-548b	3.21±3.16	0.52	1.25±1.06	0.82
hsa-miR-520f	3.20±2.25	0.38	0.94±0.57	0.92
hsa-miR-548d	2.95±2.82	0.53	0.31±0.25	N/A
hsa-miR-154	2.73±2.17	0.47	3.70±2.98	0.42
hsa-miR-489	2.73±1.58	0.34	1.47±0.66	0.52
hsa-miR-455	2.70±0.89	0.13	1.84±0.25	<0.05
hsa-miR-326	2.54±1.38	0.33	1.02±0.16	0.89
hsa-miR-589	2.53±1.44	0.35	1.97±0.58	0.17
hsa-miR-449a	2.26±1.64	0.48	3.06±2.45	0.45
hsa-miR-375	2.18±2.18	0.62	0.05±0.05	<0.05

hsa-miR-216b	2.01±0.63	0.18	0.59±0.16	0.07
hsa-miR-485-5p	2.01±1.29	0.48	0.81±0.12	0.19
hsa-miR-216a	1.82±0.83	0.38	2.49±0.25	<0.05
hsa-miR-517c	1.81±1.34	0.58	4.88±4.77	0.46
hsa-miR-409-5p	1.77±0.77	0.37	1.88±1.13	0.48
hsa-miR-483-5p	1.77±0.23	<0.05	0.95±0.19	0.80
hsa-miR-519d	1.73±0.96	0.49	2.83±2.68	0.53
hsa-miR-372	1.71±1.71	0.70	0.07±0.07	<0.05
hsa-miR-493	1.71±0.31	0.09	0.86±0.46	0.78
hsa-miR-143	1.69±0.63	0.33	1.24±0.40	0.58
hsa-miR-545	1.66±0.86	0.49	1.31±0.75	0.70
hsa-miR-211	1.61±0.53	0.31	0.77±0.21	0.34
hsa-miR-455-5p	1.55±0.28	0.12	1.32±0.32	0.37
hsa-miR-518b	1.51±0.66	0.48	1.20±0.66	0.78
hsa-miR-193a	1.49±0.56	0.44	1.17±0.24	0.52
hsa-miR-433	1.49±0.37	0.26	1.03±0.36	0.95
hsa-miR-129-3p	1.41±1.18	0.74	0.46±0.34	0.19
hsa-miR-31	1.37±0.10	<0.05	1.33±0.12	0.06
hsa-miR-296-5p	1.35±0.80	0.68	4.24±2.95	0.33
hsa-miR-212	1.32±0.25	0.27	1.13±0.35	0.74
hsa-miR-124	1.25±0.23	0.35	1.08±0.65	0.90
hsa-miR-15a	1.21±0.60	0.74	1.91±0.77	0.30
hsa-miR-224	1.21±0.19	0.33	1.41±0.23	0.15
hsa-miR-20b	1.16±0.36	0.67	1.00±0.06	0.95
hsa-miR-301b	1.15±0.38	0.72	0.95±0.08	0.59

hsa-miR-410	1.15±0.40	0.72	0.97±0.24	0.92
hsa-miR-501-5p	1.14±0.42	0.76	1.51±0.90	0.60
hsa-miR-125a	1.13±0.31	0.69	1.17±0.19	0.43
hsa-miR-148b	1.13±0.14	0.41	1.27±0.19	0.23
hsa-miR-628-5p	1.13±0.22	0.59	1.33±0.14	0.08
hsa-miR-522	1.10±0.61	0.88	0.87±0.53	0.82
RNU44	1.10±0.16	0.54	1.19±0.28	0.53
hsa-miR-217	1.07±0.26	0.79	1.21±0.25	0.45
hsa-miR-222	1.06±0.07	0.41	1.23±0.10	0.09
hsa-miR-758	1.06±0.60	0.92	2.28±0.63	0.11
hsa-let-7g	1.04±0.37	0.91	1.50±0.38	0.26
hsa-miR-134	1.04±0.07	0.58	1.00±0.14	0.99
hsa-miR-23a	1.03±0.46	0.95	1.68±0.52	0.26
hsa-miR-423-5p	1.03±0.28	0.91	0.59±0.42	0.38
hsa-miR-132	1.02±0.12	0.88	1.26±0.16	0.18
hsa-miR-139-5p	1.02±0.23	0.93	0.95±0.09	0.62
hsa-miR-145	1.02±0.15	0.92	1.24±0.07	<0.05
hsa-miR-181a	1.02±0.25	0.94	1.46±0.29	0.19
hsa-miR-28-5p	1.02±0.16	0.92	1.11±0.02	<0.05
hsa-miR-484	1.02±0.10	0.83	1.17±0.12	0.22
hsa-miR-324-5p	1.01±0.32	0.98	1.02±0.22	0.93
hsa-miR-331-5p	1.01±0.23	0.97	1.72±0.88	0.46
hsa-miR-337-5p	1.01±0.32	0.98	1.37±0.14	0.06
hsa-miR-425	1.01±0.12	0.94	1.34±0.47	0.51
hsa-miR-500	1.01±0.40	0.98	1.59±0.34	0.16

hsa-miR-517b	1.01±0.55	0.99	7.24±4.21	0.21
hsa-miR-886-3p	1.01±0.12	0.96	1.02±0.08	0.82
hsa-miR-886-5p	1.01±0.08	0.94	1.24±0.13	0.15
hsa-miR-431	1.00±0.26	0.99	1.85±0.50	0.16
hsa-miR-320	0.99±0.15	0.97	1.13±0.16	0.46
hsa-miR-24	0.98±0.12	0.87	1.20±0.13	0.20
hsa-miR-339-3p	0.97±0.15	0.83	0.97±0.14	0.84
hsa-miR-218	0.96±0.16	0.82	1.44±0.12	<0.05
hsa-miR-521	0.96±0.54	0.94	0.62±0.38	0.37
RNU48	0.96±0.03	0.26	1.02±0.15	0.88
hsa-miR-146b	0.95±0.22	0.83	1.03±0.23	0.91
hsa-miR-186	0.95±0.12	0.70	1.18±0.06	<0.05
hsa-miR-193b	0.95±0.08	0.52	1.13±0.12	0.34
hsa-miR-19a	0.95±0.33	0.88	1.75±0.64	0.31
hsa-miR-200b	0.95±0.44	0.91	2.39±1.29	0.34
hsa-miR-34a	0.95±0.25	0.84	1.55±0.08	<0.05
hsa-miR-454	0.95±0.11	0.69	1.09±0.21	0.69
hsa-miR-541	0.95±0.95	0.96	0.48±0.48	0.34
hsa-miR-574-3p	0.95±0.06	0.44	1.11±0.17	0.56
hsa-miR-655	0.95±0.37	0.89	2.04±0.43	0.07
hsa-miR-28-3p	0.94±0.05	0.29	1.12±0.04	<0.05
hsa-let-7f	0.93±0.13	0.63	1.72±0.37	0.12
hsa-miR-139-3p	0.93±0.75	0.93	3.32±3.09	0.49
hsa-miR-182	0.93±0.93	0.94	0.12±0.12	<0.05
hsa-miR-323-3p	0.93±0.01	<0.05	1.33±0.20	0.18

hsa-miR-369-3p	0.93±0.07	0.37	3.96±2.30	0.27
hsa-miR-376c	0.93±0.12	0.58	1.38±0.34	0.32
hsa-miR-93	0.93±0.11	0.57	1.10±0.08	0.29
hsa-miR-127-3p	0.92±0.23	0.75	1.04±0.04	0.40
hsa-miR-17	0.92±0.10	0.46	1.28±0.20	0.24
hsa-miR-193a	0.92±0.10	0.49	1.34±0.24	0.22
hsa-miR-195	0.92±0.14	0.60	1.40±0.15	0.06
hsa-miR-452	0.92±0.10	0.47	1.07±0.15	0.69
hsa-miR-187	0.91±0.42	0.84	0.81±0.51	0.73
hsa-miR-539	0.91±0.12	0.52	1.07±0.14	0.63
hsa-miR-629	0.91±0.46	0.86	1.05±0.57	0.94
hsa-miR-99b	0.91±0.12	0.49	1.20±0.12	0.18
hsa-miR-342-3p	0.90±0.19	0.64	1.35±0.60	0.59
hsa-miR-494	0.90±0.17	0.61	0.92±0.06	0.25
hsa-miR-660	0.90±0.18	0.61	1.31±0.18	0.17
hsa-miR-223	0.89±0.10	0.31	0.86±0.07	0.12
hsa-miR-744	0.89±0.22	0.64	1.03±0.16	0.84
hsa-miR-18b	0.88±0.22	0.60	1.29±0.29	0.38
hsa-miR-21	0.88±0.20	0.59	1.70±0.77	0.42
hsa-miR-422a	0.88±0.46	0.81	6.22±3.38	0.20
hsa-let-7a	0.87±0.44	0.78	2.54±1.08	0.23
hsa-miR-191	0.87±0.11	0.32	1.11±0.10	0.34
hsa-miR-301a	0.87±0.20	0.56	1.28±0.21	0.25
hsa-miR-331-3p	0.87±0.02	<0.05	1.17±0.19	0.42
hsa-miR-520e	0.87±0.87	0.89	0.13±0.13	<0.05

hsa-miR-106a	0.86±0.05	0.06	1.38±0.17	0.09
hsa-miR-130b	0.86±0.20	0.53	1.35±0.18	0.13
hsa-miR-18a	0.86±0.20	0.52	1.38±0.13	<0.05
hsa-miR-365	0.86±0.10	0.25	1.22±0.11	0.13
hsa-miR-130a	0.85±0.35	0.69	1.86±0.52	0.18
hsa-miR-140-3p	0.85±0.33	0.67	1.44±0.60	0.50
hsa-miR-142-3p	0.85±0.39	0.72	14.4±11.55	0.31
hsa-miR-29a	0.85±0.24	0.55	1.37±0.11	<0.05
hsa-miR-329	0.85±0.54	0.79	0.98±0.33	0.95
hsa-miR-330-3p	0.85±0.08	0.14	1.39±0.31	0.27
hsa-miR-487a	0.85±0.28	0.63	2.09±0.61	0.15
hsa-miR-106b	0.84±0.15	0.35	1.43±0.14	<0.05
hsa-miR-150	0.84±0.04	<0.05	1.81±0.43	0.14
hsa-miR-23b	0.84±0.17	0.40	1.30±0.31	0.39
hsa-miR-29c	0.84±0.18	0.42	1.64±0.27	0.08
hsa-miR-376a	0.84±0.22	0.50	1.49±0.60	0.46
hsa-miR-532-5p	0.84±0.11	0.21	1.25±0.10	0.06
hsa-miR-29b	0.83±0.11	0.20	2.05±0.30	<0.05
hsa-miR-339-5p	0.83±0.03	<0.05	1.07±0.35	0.84
hsa-miR-382	0.83±0.11	0.20	1.19±0.40	0.66
hsa-miR-485-3p	0.83±0.10	0.16	0.68±0.06	<0.05
hsa-miR-103	0.82±0.10	0.15	1.47±0.30	0.19
hsa-miR-181c	0.82±0.44	0.71	1.37±0.36	0.36
hsa-miR-328	0.82±0.22	0.45	1.03±0.11	0.79
hsa-miR-486-5p	0.82±0.22	0.45	0.45±0.10	<0.05

hsa-miR-487b	0.82±0.09	0.11	1.37±0.24	0.20
hsa-miR-518f	0.82±0.82	0.83	0.14±0.14	<0.05
hsa-miR-197	0.81±0.05	<0.05	1.02±0.34	0.96
hsa-miR-491-5p	0.81±0.09	0.09	1.11±0.13	0.45
hsa-miR-100	0.80±0.20	0.38	1.18±0.11	0.16
hsa-miR-20a	0.80±0.08	0.06	1.54±0.16	<0.05
hsa-miR-25	0.80±0.09	0.10	1.41±0.09	<0.05
hsa-miR-576-3p	0.80±0.28	0.51	1.13±0.42	0.78
hsa-miR-598	0.80±0.31	0.56	1.18±0.14	0.26
hsa-miR-590-5p	0.79±0.15	0.23	1.48±0.19	0.06
hsa-miR-889	0.79±0.23	0.41	1.46±0.16	<0.05
hsa-miR-324-3p	0.78±0.20	0.34	1.35±0.09	<0.05
hsa-miR-411	0.78±0.11	0.13	1.54±0.44	0.29
hsa-miR-449b	0.78±0.30	0.51	1.02±0.35	0.96
hsa-miR-19b	0.77±0.16	0.21	1.41±0.16	0.06
hsa-miR-345	0.77±0.15	0.22	0.98±0.14	0.91
hsa-miR-361-5p	0.77±0.28	0.46	1.39±0.35	0.33
hsa-miR-495	0.77±0.10	0.07	1.08±0.12	0.53
hsa-miR-107	0.76±0.52	0.67	0.33±0.18	<0.05
hsa-miR-340	0.76±0.27	0.41	1.76±0.45	0.16
hsa-miR-532-3p	0.76±0.07	<0.05	1.07±0.05	0.25
hsa-miR-887	0.76±0.26	0.39	3.12±2.46	0.44
hsa-miR-374a	0.75±0.16	0.19	1.57±0.24	0.07
hsa-miR-26b	0.74±0.15	0.16	1.62±0.23	0.06
hsa-miR-92a	0.74±0.04	<0.05	1.34±0.20	0.17

hsa-miR-140-5p	0.73±0.15	0.15	1.26±0.15	0.17
hsa-miR-505	0.73±0.34	0.47	4.77±3.41	0.33
hsa-miR-519a	0.73±0.61	0.68	2.63±2.28	0.52
hsa-miR-576-5p	0.73±0.27	0.37	1.98±0.73	0.25
hsa-miR-127-5p	0.72±0.28	0.37	3.10±1.21	0.16
hsa-miR-16	0.72±0.16	0.16	1.24±0.20	0.29
hsa-miR-221	0.72±0.18	0.20	1.36±0.15	0.08
hsa-miR-26a	0.72±0.15	0.14	1.49±0.19	0.06
hsa-miR-362-5p	0.72±0.36	0.47	1.14±0.25	0.59
hsa-miR-542-3p	0.72±0.40	0.52	3.54±2.90	0.43
hsa-miR-214	0.71±0.06	<0.05	1.15±0.06	0.06
hsa-miR-519e	0.71±0.56	0.63	1.38±0.24	0.18
hsa-miR-10a	0.69±0.11	<0.05	1.39±0.07	<0.05
hsa-miR-126	0.69±0.11	<0.05	1.60±0.33	0.15
hsa-miR-192	0.69±0.18	0.17	1.36±0.23	0.20
hsa-miR-196b	0.69±0.07	<0.05	1.39±0.04	<0.05
hsa-miR-302c	0.69±0.58	0.62	0.45±0.23	0.08
hsa-miR-379	0.69±0.15	0.10	1.36±0.23	0.20
hsa-miR-517a	0.69±0.38	0.46	0.32±0.23	<0.05
hsa-miR-125b	0.68±0.14	0.09	1.31±0.25	0.28
hsa-miR-299-5p	0.68±0.05	<0.05	1.48±0.57	0.45
hsa-miR-652	0.68±0.11	<0.05	1.42±0.26	0.18
hsa-let-7b	0.67±0.13	0.06	1.45±0.25	0.14
hsa-miR-27a	0.67±0.12	<0.05	2.01±0.32	<0.05
hsa-miR-374b	0.67±0.09	<0.05	1.38±0.16	0.07

hsa-miR-15b	0.66±0.10	<0.05	1.75±0.49	0.20
hsa-miR-363	0.66±0.26	0.27	5.53±2.70	0.17
hsa-miR-671-3p	0.66±0.24	0.23	1.61±0.43	0.23
hsa-miR-874	0.66±0.13	<0.05	1.15±0.16	0.38
hsa-miR-10b	0.65±0.09	<0.05	1.37±0.18	0.10
hsa-let-7e	0.64±0.11	<0.05	2.13±0.40	<0.05
hsa-miR-125a	0.64±0.21	0.17	1.28±0.08	<0.05
hsa-miR-194	0.64±0.17	0.10	2.58±0.87	0.14
hsa-miR-199a	0.64±0.13	<0.05	1.66±0.21	<0.05
hsa-let-7c	0.63±0.13	<0.05	1.65±0.13	<0.05
hsa-miR-128	0.63±0.06	<0.05	1.41±0.25	0.18
hsa-miR-204	0.63±0.19	0.12	1.82±0.59	0.24
hsa-miR-27b	0.62±0.14	<0.05	1.41±0.27	0.20
hsa-miR-370	0.62±0.13	<0.05	1.36±0.34	0.36
hsa-miR-450b	0.62±0.29	0.26	4.04±1.32	0.08
hsa-miR-148a	0.61±0.07	<0.05	1.47±0.42	0.33
hsa-let-7d	0.60±0.09	<0.05	1.73±0.10	<0.05
hsa-miR-152	0.60±0.08	<0.05	1.82±0.40	0.11
hsa-miR-210	0.59±0.06	<0.05	1.39±0.15	0.06
hsa-miR-22	0.59±0.23	0.16	4.10±3.13	0.38
hsa-miR-625	0.59±0.16	0.07	1.87±0.84	0.36
hsa-miR-185	0.58±0.08	<0.05	1.70±0.31	0.08
hsa-miR-501-3p	0.58±0.30	0.23	15.54±14.43	0.37
hsa-miR-502-3p	0.57±0.07	<0.05	2.08±0.60	0.15
hsa-miR-636	0.57±0.15	<0.05	2.14±1.15	0.38

hsa-miR-486-3p	0.56±0.19	0.08	1.05±0.40	0.90
hsa-miR-518d	0.56±0.36	0.28	6.12±5.96	0.44
hsa-miR-335	0.55±0.13	<0.05	1.09±0.47	0.85
hsa-miR-135a	0.54±0.25	0.14	1.90±0.53	0.17
hsa-miR-205	0.54±0.54	0.44	0.21±0.21	<0.05
hsa-miR-99a	0.54±0.14	<0.05	1.30±0.24	0.27
hsa-miR-203	0.52±0.12	<0.05	2.13±0.75	0.20
hsa-miR-101	0.51±0.11	<0.05	2.12±0.06	<0.05
hsa-miR-424	0.47±0.25	0.10	3.76±2.74	0.37
hsa-miR-95	0.47±0.30	0.28	1.27±0.27	0.37
hsa-miR-515-3p	0.46±0.29	0.14	1.89±1.37	0.55
hsa-miR-579	0.46±0.23	0.08	10.36±10.32	0.42
hsa-miR-523	0.45±0.12	0.14	10.46±7.02	0.25
hsa-miR-1	0.43±0.43	0.25	0.52±0.52	0.40
hsa-miR-32	0.43±0.29	0.12	26.15±24.01	0.35
hsa-miR-215	0.40±0.22	0.06	2.40±0.77	0.14
hsa-miR-519c	0.40±0.40	0.21	0.28±0.28	0.06
hsa-miR-653	0.40±0.40	0.21	0.39±0.39	0.19
has-miR-155	0.39±0.28	0.13	1.78±0.69	0.32
hsa-miR-627	0.38±0.31	0.12	9.11±8.73	0.41
hsa-miR-199a	0.37±0.32	0.12	17.88±12.74	0.26
hsa-miR-190	0.35±0.21	0.12	6.58±3.87	0.22
hsa-miR-582-3p	0.35±0.32	0.12	5.53±3.25	0.24
hsa-miR-654-5p	0.35±0.26	0.07	9.55±8.94	0.39
hsa-miR-105	N/A		N/A	

hsa-miR-122	N/A	N/A	
hsa-miR-129-5p	N/A	N/A	
hsa-miR-133b	N/A	N/A	
hsa-miR-136	N/A	N/A	
hsa-miR-142-5p	N/A	0.72±0.36	0.49
hsa-miR-147	N/A	N/A	
hsa-miR-147b	N/A	N/A	
hsa-miR-153	N/A	N/A	
hsa-miR159a	N/A	N/A	
hsa-miR-183	N/A	N/A	
hsa-miR-188-3p	N/A	N/A	
hsa-miR-198	N/A	3.25±3.25	0.53
hsa-miR-200c	N/A	19.7±9.91	0.13
hsa-miR-208	N/A	N/A	
hsa-miR-208b	N/A	N/A	
hsa-miR-219	N/A	N/A	
hsa-miR-219	N/A	N/A	
hsa-miR-219-5p	N/A	N/A	
hsa-miR-220	N/A	N/A	
hsa-miR-220b	N/A	N/A	
hsa-miR-220c	N/A	N/A	
hsa-miR-296-3p	N/A	N/A	
hsa-miR-298	N/A	N/A	
hsa-miR-299-3p	N/A	14.43±13.3	0.37
hsa-miR-302a	N/A	N/A	

hsa-miR-302b	N/A	N/A	
hsa-miR-325	N/A	N/A	
hsa-miR-338-3p	N/A	N/A	
hsa-miR-33b	N/A	8.67±8.67	0.43
hsa-miR-342-5p	N/A	0.33±0.33	0.12
hsa-miR-34c-5p	N/A	N/A	
hsa-miR-362-3p	N/A	3.48±2.09	0.30
hsa-miR-367	N/A	N/A	
hsa-miR-371-3p	N/A	N/A	
hsa-miR-373	N/A	2.13±2.13	0.62
hsa-miR-376b	N/A	1.52±1.14	0.67
hsa-miR-377	N/A	N/A	
hsa-miR-383	N/A	N/A	
hsa-miR-384	N/A	N/A	
hsa-miR-412	N/A	N/A	
hsa-miR-448	N/A	N/A	
hsa-miR-450b	N/A	N/A	
hsa-miR-453	N/A	N/A	
hsa-miR-488	N/A	N/A	
hsa-miR-490-3p	N/A	N/A	
hsa-miR-491-3p	N/A	N/A	
hsa-miR-492	N/A	N/A	
hsa-miR-496	N/A	N/A	
hsa-miR-499-3p	N/A	N/A	
hsa-miR-499-5p	N/A	N/A	

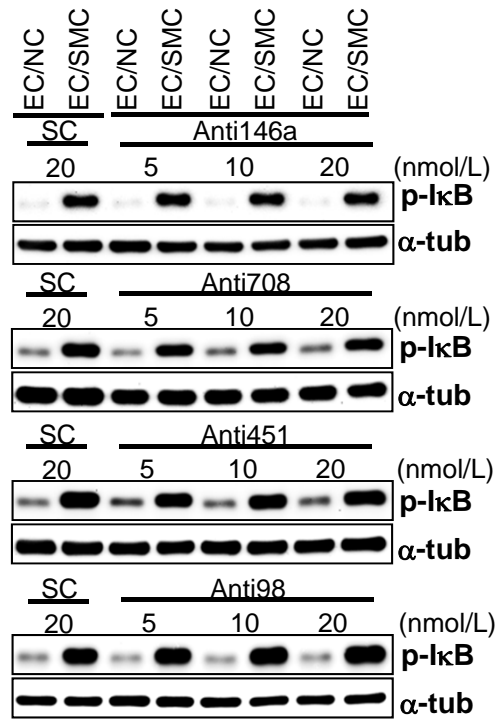
hsa-miR-504	N/A	N/A
hsa-miR-506	N/A	N/A
hsa-miR-507	N/A	N/A
hsa-miR-508-5p	N/A	N/A
hsa-miR-509	N/A	N/A
hsa-miR-509-5p	N/A	N/A
hsa-miR-510	N/A	N/A
hsa-miR-511	N/A	N/A
hsa-miR-512-3p	N/A	N/A
hsa-miR-512-5p	N/A	N/A
hsa-miR-513-5p	N/A	N/A
hsa-miR-515-5p	N/A	N/A
hsa-miR-516a	N/A	N/A
hsa-miR-516b	N/A	N/A
hsa-miR-518a	N/A	N/A
hsa-miR-518a	N/A	N/A
hsa-miR-518c	N/A	N/A
hsa-miR-518d	N/A	N/A
hsa-miR-520a	N/A	N/A
hsa-miR-520a	N/A	N/A
hsa-miR-520b	N/A	N/A
hsa-miR-520d	N/A	N/A
hsa-miR-524-5p	N/A	N/A
hsa-miR-525-3p	N/A	N/A
hsa-miR-525-5p	N/A	N/A

hsa-miR-526b	N/A	N/A	
hsa-miR-542-5p	N/A	1.95±1.28	0.50
hsa-miR-544	N/A	N/A	
hsa-miR-548a	N/A	N/A	
hsa-miR-548a	N/A	N/A	
hsa-miR-548b	N/A	N/A	
hsa-miR-548c	N/A	N/A	
hsa-miR-548c	N/A	N/A	
hsa-miR-548d	N/A	N/A	
hsa-miR-551b	N/A	N/A	
hsa-miR-556-3p	N/A	N/A	
hsa-miR-556-5p	N/A	N/A	
hsa-miR-561	N/A	N/A	
hsa-miR-570	N/A	N/A	
hsa-miR-615-3p	N/A	N/A	
hsa-miR-615-5p	N/A	N/A	
hsa-miR-616	N/A	N/A	
hsa-miR-618	N/A	N/A	
hsa-miR-624	N/A	N/A	
hsa-miR-642	N/A	N/A	
hsa-miR-651	N/A	N/A	
hsa-miR-672	N/A	N/A	
hsa-miR-674	N/A	N/A	
hsa-miR-871	N/A	N/A	
hsa-miR-872	N/A	N/A	

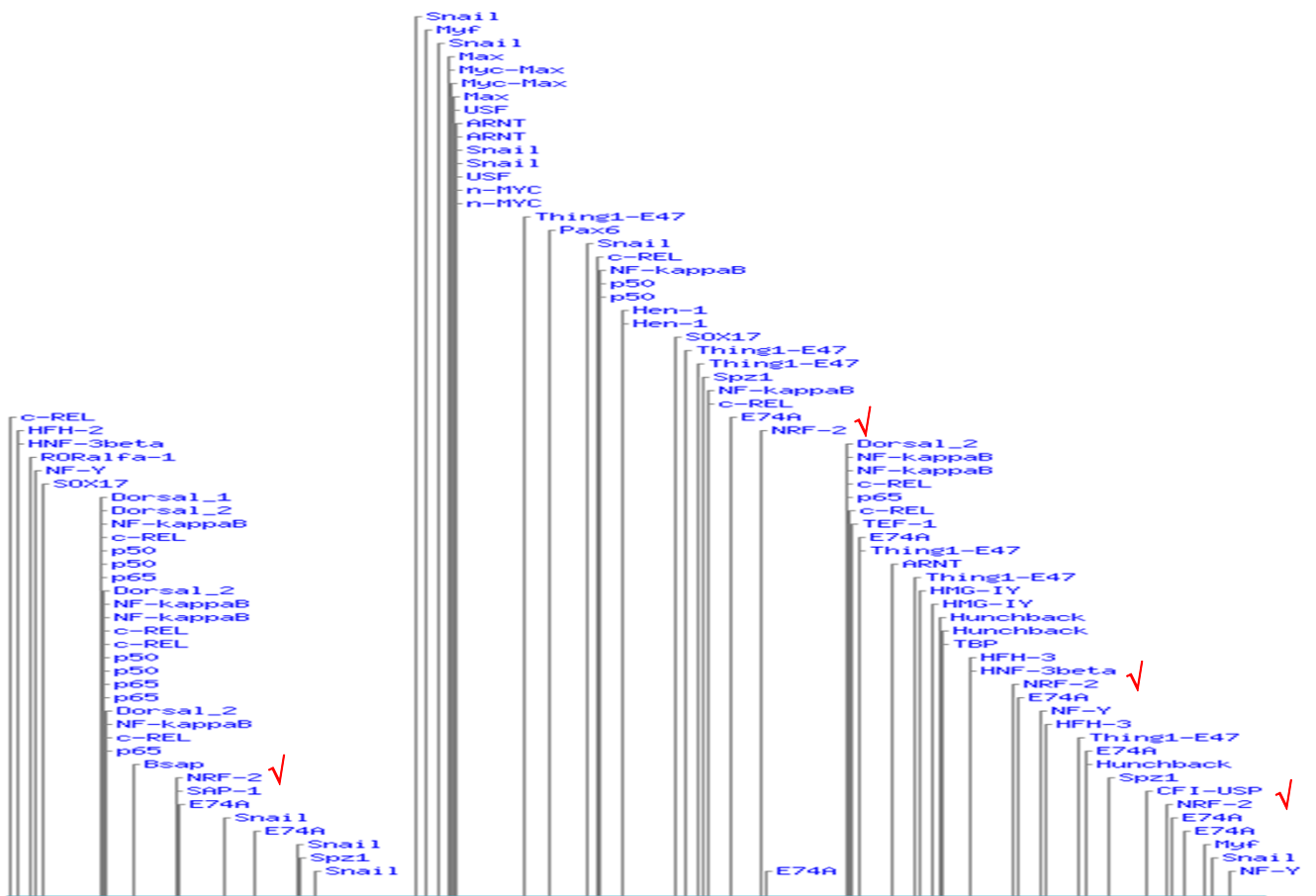
hsa-miR-873	N/A	N/A	
hsa-miR-875-3p	N/A	N/A	
hsa-miR-876-3p	N/A	N/A	
hsa-miR-876-5p	N/A	N/A	
hsa-miR-885-3p	N/A	N/A	
hsa-miR-888	N/A	0.65±0.34	0.36
hsa-miR-890	N/A	N/A	
hsa-miR-891a	N/A	N/A	
hsa-miR-891b	N/A	N/A	
hsa-miR-892a	N/A	N/A	
hsa-miR-96	N/A	N/A	

Data are mean±SEM from three independent experiments. N/A: not available: data of at least one experiment cannot be detected. *: a mean co-culture/monoculture ratio ≥ 2.0 and $P \leq 0.05$. **: a mean co-culture/monoculture ratio ≤ 0.5 and $P \leq 0.05$.

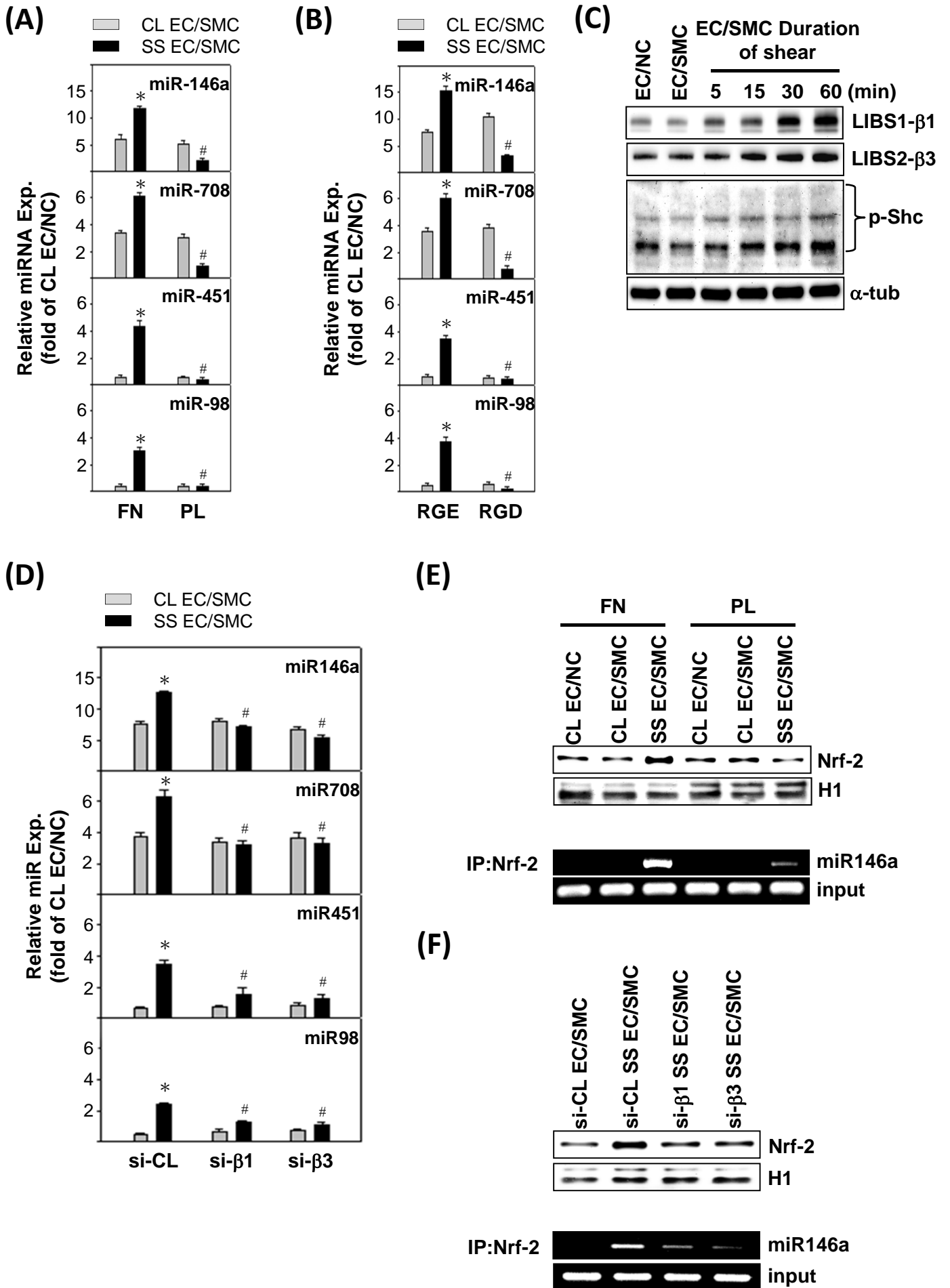
Online Figure II



Online Figure III

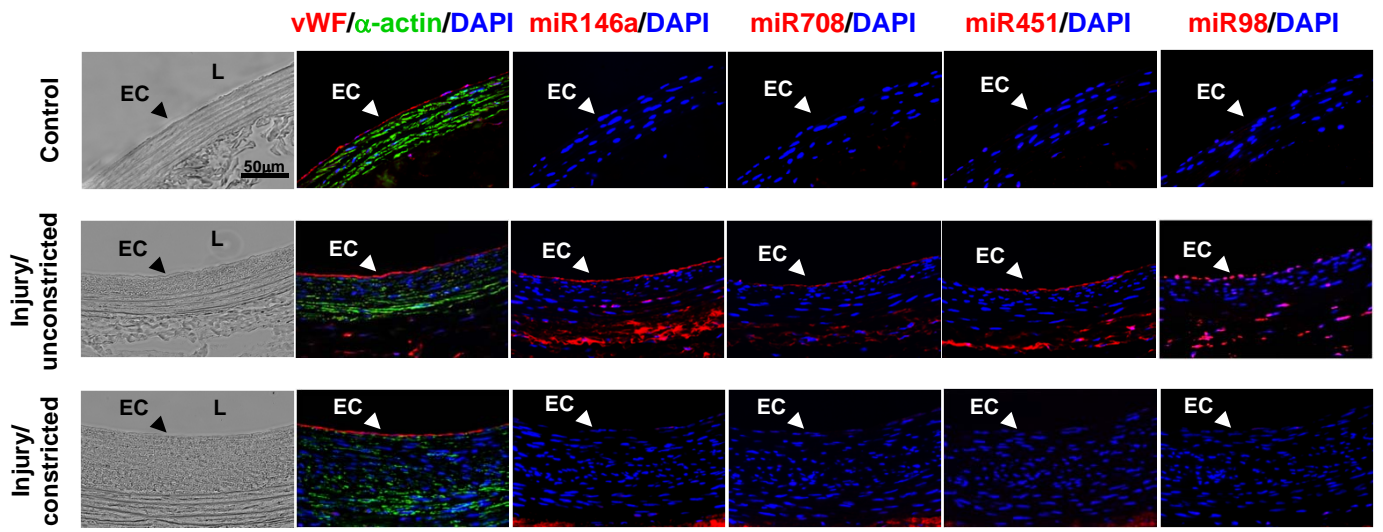


Online Figure IV

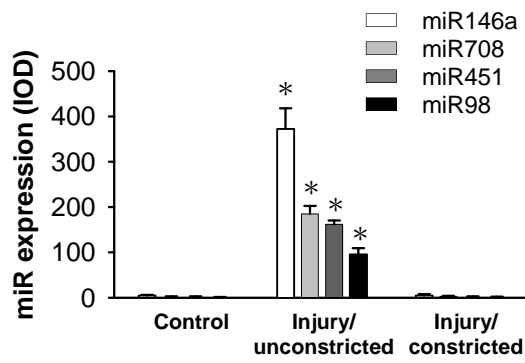


Online Figure V

(A)

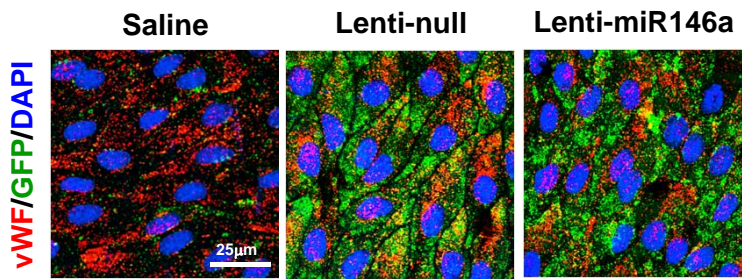


(B)

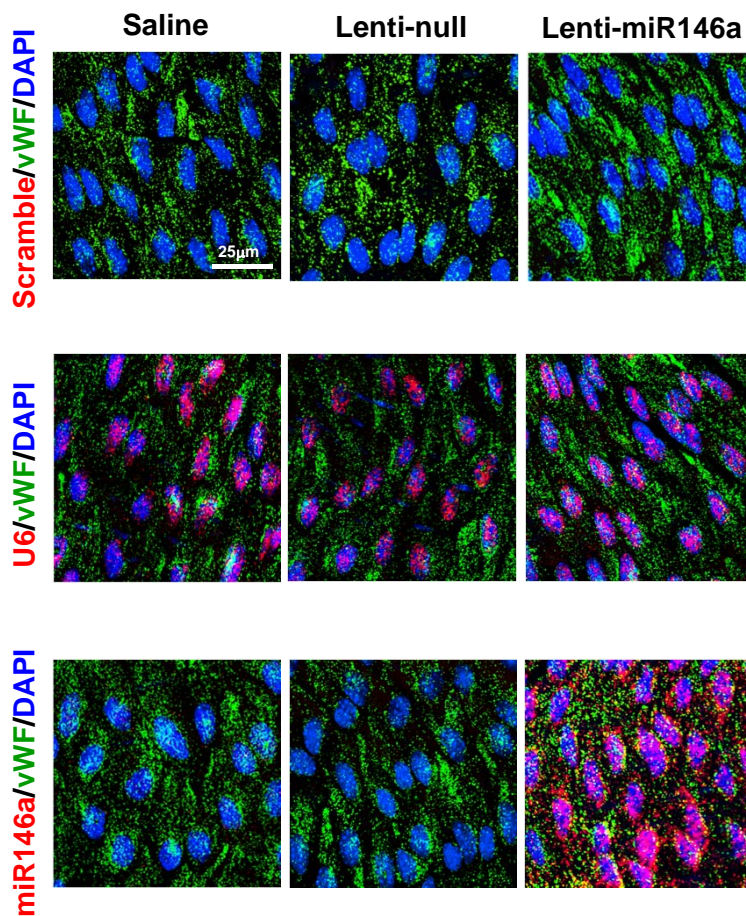


Online Figure VI

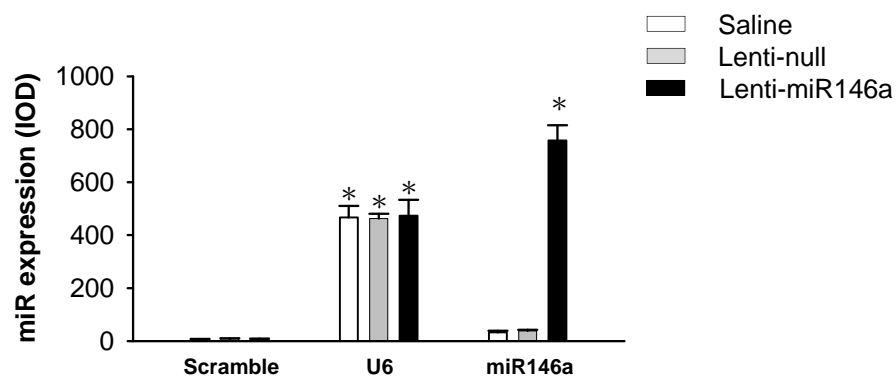
(A)



(B)

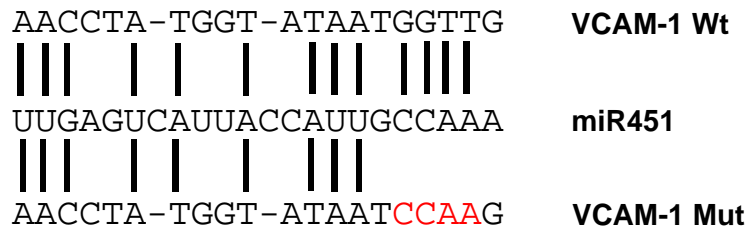


(C)

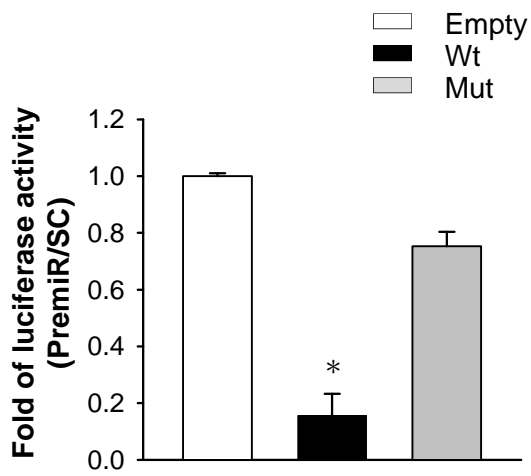


Online Figure VII

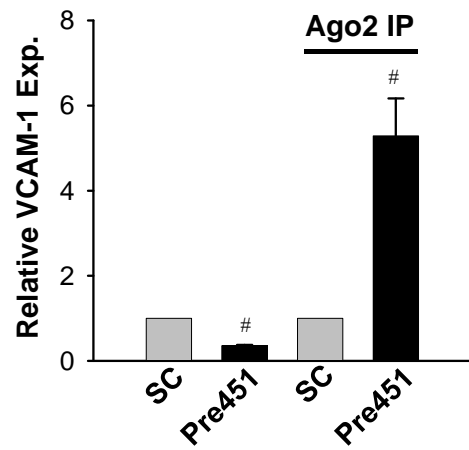
(A)



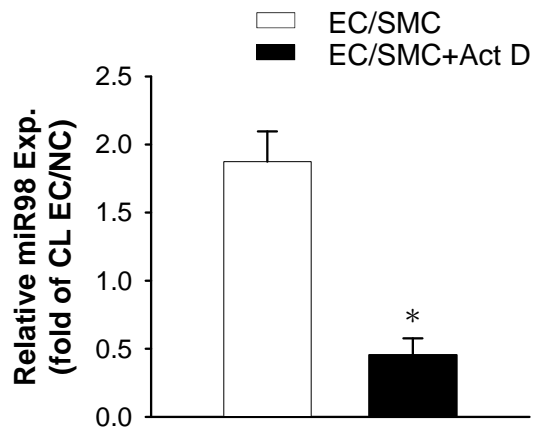
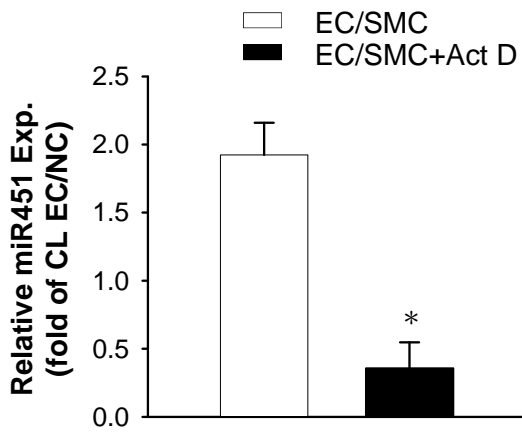
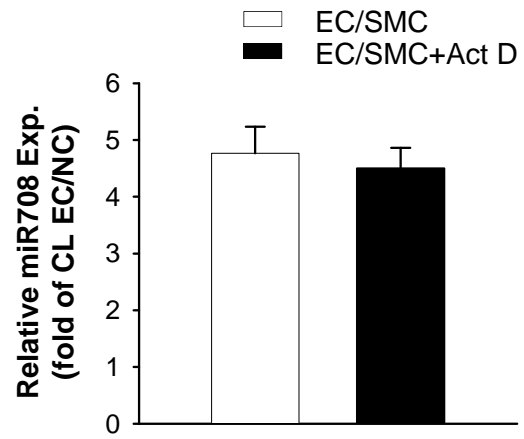
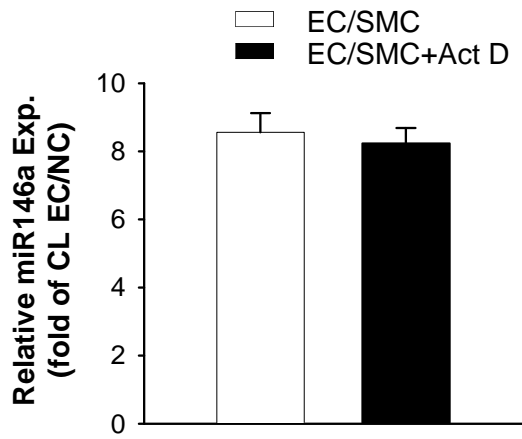
(B)



(C)

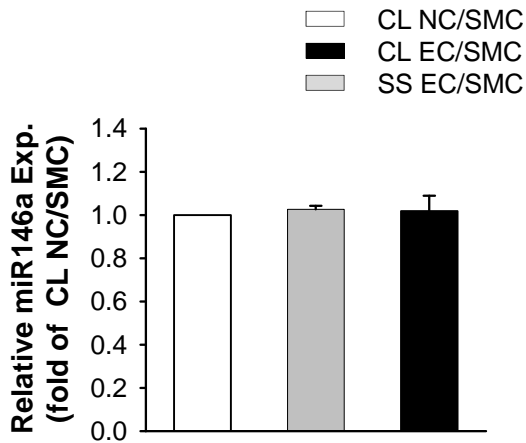


Online Figure VIII

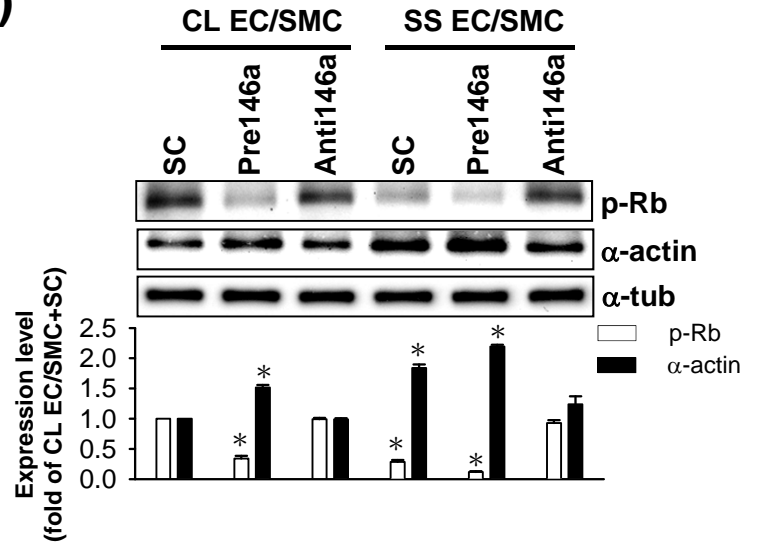


Online Figure IX

(A)



(B)



Circulation Research

JOURNAL OF THE AMERICAN HEART ASSOCIATION



MicroRNA Mediation of Endothelial Inflammatory Response to Smooth Muscle Cells and Its Inhibition by Atheroprotective Shear Stress

Li-Jing Chen, Li Chuang, Yi-Hsuan Huang, Jing Zhou, Seh Hong Lim, Chih-I Lee, Wei-Wen Lin, Ting-Er Lin, Wei-Li Wang, Linyi Chen, Shu Chien and Jeng-Jiann Chiu

Circ Res. 2015;116:1157-1169; originally published online January 26, 2015;
doi: 10.1161/CIRCRESAHA.116.305987

Circulation Research is published by the American Heart Association, 7272 Greenville Avenue, Dallas, TX 75231
Copyright © 2015 American Heart Association, Inc. All rights reserved.
Print ISSN: 0009-7330. Online ISSN: 1524-4571

The online version of this article, along with updated information and services, is located on the World Wide Web at:

<http://circres.ahajournals.org/content/116/7/1157>

Data Supplement (unedited) at:

<http://circres.ahajournals.org/content/suppl/2015/01/26/CIRCRESAHA.116.305987.DC1.html>

Permissions: Requests for permissions to reproduce figures, tables, or portions of articles originally published in *Circulation Research* can be obtained via RightsLink, a service of the Copyright Clearance Center, not the Editorial Office. Once the online version of the published article for which permission is being requested is located, click Request Permissions in the middle column of the Web page under Services. Further information about this process is available in the [Permissions and Rights Question and Answer](#) document.

Reprints: Information about reprints can be found online at:
<http://www.lww.com/reprints>

Subscriptions: Information about subscribing to *Circulation Research* is online at:
<http://circres.ahajournals.org/subscriptions/>